

1 **Dynamics and dispersion modelling of nanoparticles from road traffic in**
2 **the urban atmospheric environment – a review**

3 **Prashant Kumar^{a,b,*}, Matthias Ketznel^c, Sotiris Vardoulakis^d, Liisa Pirjola^e, Rex Britter^f**

4 ^a*Division of Civil, Chemical and Environmental Engineering, Faculty of Engineering and*
5 *Physical Sciences (FEPS), University of Surrey, Guildford GU2 7XH, United Kingdom*

6 ^b*Environmental Flow (EnFlo) Research Centre, FEPS, University of Surrey, Guildford GU2*
7 *7XH, United Kingdom*

8 ^c*Department of Environmental Science, Aarhus University, DK-4000 Roskilde, Denmark*

9 ^d*Centre for Radiation, Chemical & Environmental Hazards, Health Protection Agency,*
10 *Chilton OX11 0RQ, United Kingdom*

11 ^e*Department of Physics, University of Helsinki, FI-00064 Helsinki, Finland, and Department*
12 *of Technology, Metropolia University of Applied Sciences, FI-00180 Helsinki, Finland*

13 ^f*Senseable City Laboratory, Massachusetts Institute of Technology, Boston, MA 02139, USA*
14

15 **Abstract**

16 Reducing exposure to atmospheric nanoparticles in urban areas is important for
17 protecting public health. Developing new or improving the capabilities of existing
18 dispersion models will help to design effective mitigation strategies for nanoparticle
19 rich environments. The aims of this review are to summarise current practices of
20 nanoparticle dispersion modelling at five local scales (i.e. vehicle wake, street
21 canyons, neighbourhood, city and road tunnels), together with highlighting associated
22 challenges, research gaps and priorities. The review begins with a synthesis of
23 available information about the flow and mixing characteristics in urban environments
24 which is followed by a brief discussion on dispersion modelling of nanoparticles.
25 Further sections cover the effects of transformation processes in dispersion modelling
26 of nanoparticles, and a critical discussion on associated structural and parametric
27 uncertainties in modelling. The article concludes with a comprehensive summary of
28 current knowledge and future research required on the topic areas covered.

29 Appropriate treatment of transformation processes (i.e. nucleation, coagulation,
30 deposition and condensation) in existing dispersion models is essential for extending
31 the applicability of gaseous dispersion models to nanoparticles. Some modelling
32 studies that consider the particles down to 1 nm size indicate importance of
33 coagulation and condensation processes on street-scale modelling whereas others
34 neglecting either sub-10 nm particles or Van der Waals forces along with fractal
35 geometry suggest to discard these processes due to negligible effects on particle
36 number and size distributions. Further, it is important to consider those transformation
37 processes e.g. at city scale or in road tunnels because of the much longer residence
38 time or much higher concentration levels compared to the street scale processes.
39 Structural and parametric uncertainties affect the modelled results considerably. In
40 particular, parametric uncertainty in the form of particle number emission factors
41 appears to be the most significant due to considerably large variations in their
42 estimates. A consistent approach to the use of emission factors, appropriate treatment
43 of transformation processes in particle dispersion models and the evaluation of model

* Corresponding author: Civil Engineering (C5), University of Surrey, Guildford GU2 7XH, UK; Tel.: +44 1483 682762; Fax: +44 1483 682135.

Email addresses: P.Kumar@surrey.ac.uk or Prashant.Kumar@cantab.net

44 performance against measured data are essential for producing reliable modelled
45 results.

46 **Key words:** Aerosol and particle dispersion; Model uncertainty; Nanoparticle
47 modelling; Number and size distribution; Street canyon; Ultrafine particles
48

49 1. Introduction

50 Nanoparticle emissions from road vehicles and their adverse impacts on human
51 health and environment have urged the air quality science and management
52 communities to reinforce research in this area. While emission sources such as power
53 plants (Li et al., 2009), airports (Hu et al., 2009), building demolition sites (Hansen et
54 al., 2008), tyre and road surface wear (Dahl et al., 2006), biofuel derived (Kumar et
55 al., 2010b), natural formation (Holmes, 2007) and other emerging sources such as
56 manufactured nanomaterials (Kumar et al., 2010a) are important contributors to the
57 *number* concentration of atmospheric particles, emissions from gasoline- and diesel-
58 fuelled vehicles remain the dominant source in polluted urban environments. These
59 can alone contribute up to about 90% of the total particle number (ToN)
60 concentrations (Pey et al., 2009).

61 Atmospheric nanoparticles need to be controlled for several reasons: the toxic nature
62 of fresh emissions (Murr and Garza, 2009), the ability of ultrafine fraction particles
63 (<100 nm) to penetrate the epithelial cells and accumulate in lymph nodes (Nel et al.,
64 2006), the possible association with paediatric asthma (Andersen et al., 2008) and the
65 potential for oxidative damage to DNA which may lead to increased risk of cancer
66 (Møller et al., 2008) are a few examples of adverse health effects to the public due to
67 nanoparticle exposure. Although most epidemiological studies have focused on PM₁₀
68 or PM_{2.5}, there is a certain evidence indicating that short-term exposure to high
69 concentrations of nanoparticles may aggravate existing pulmonary and cardiovascular
70 disease or trigger stroke, while long-term exposure may increase the risk of
71 cardiovascular disease and death (Andersen et al., 2010; Brugge et al., 2007; Pope III
72 and Dockery, 2006). For instance, Kumar et al. (2011a) made preliminary estimates of
73 nanoparticle emissions from road vehicles and their exposure related excess deaths in
74 megacity Delhi. They reported that exposure to ambient ToN concentrations may
75 result in a notable number of excess deaths (e.g., ~508 and ~1888 deaths per million
76 people in 2010 and 2030, respectively, under the business as usual scenario). Physico-
77 chemical characteristics of nanoparticles and their dynamic nature play an important
78 role in changing the optical properties of coarse particles in the atmosphere through
79 coagulation or condensation, leading to concerns such as diminishing urban visibility
80 (Horvath, 1994) and global climate change (Strawa et al., 2010). A comprehensive
81 review of nanoparticle characteristics, sources, measurement methodologies, health,
82 environmental and regulatory implications can be found in Kumar et al. (2010c).

83 An urban area consists of street canyons where pollutant concentrations can be several
84 times higher than in unobstructed locations depending upon traffic characteristics,
85 street canyon geometry, entrainment of emissions from adjacent streets and turbulence
86 induced by prevailing winds, traffic and atmospheric stability (Kumar et al., 2008b;
87 Kumar et al., 2009a). Real-time continuous measurements of nanoparticles at many
88 locations is rarely possible due to practical and technical constraints (Kumar et al.,

89 2011b). Therefore, a better understanding of dispersion modelling and the associated
90 challenges is crucial for designing long– or short–term mitigation strategies.

91 As seen in Fig. 1, traffic emissions in urban areas generally occur within the urban
92 canopy layer where the atmospheric flow is heavily disturbed by buildings and
93 obstacles (COST732, 2010). This leads to varying flow and dispersion characteristics
94 of pollutants in different urban settings (Britter and Hanna, 2003), and in turn
95 influencing the dilution of those emissions. When nanoparticles and their dynamics
96 are considered for dispersion modelling, dilution remains a very crucial process and it
97 is additionally accompanied by transformation processes such as nucleation,
98 coagulation, condensation, evaporation and also deposition (Ketzler et al., 2007).
99 Occurrence of these processes just after the release of emissions from vehicle tailpipes
100 in the atmosphere continuously change the number and size distributions of
101 nanoparticles and makes their dispersion modelling challenging and distinct from that
102 for gaseous air pollutants. There is currently limited and partly contradicting
103 information available on the effects of transformation processes in nanoparticle
104 dispersion models. One of the main objectives of this article is to discuss them in
105 some detail.

106 Section 3 summarises a number of reviews available on the dispersion modelling of
107 air pollutants at different urban scales. The main focus of these reviews has been on
108 gaseous pollutants or on various fractions of particulate matter on a mass basis, but
109 dispersion modelling of nanoparticles is generally not covered. This review focuses
110 on dispersion modelling of the number and size distributions of nanoparticles at five
111 urban scales. Considering that there is plenty of information already available on flow
112 characteristics and pollutant transport in different urban settings, this article discusses
113 these topics only very briefly (see Sections 2 and 3) but covers the effect of particle
114 dynamics in the dispersion modelling of *number concentrations* in detail (see Section
115 4). Furthermore, we discuss the uncertainties in the dispersion modelling of
116 nanoparticles (Section 5), which is followed by conclusions and discussions on future
117 research required on the topic areas covered.

118 The discussions presented in this article cover the following five local scales: (i)
119 vehicle wake scale, (ii) street scale, (iii) neighbourhood scale, (iv) city scale, and (v)
120 road tunnels. The focus remains on the modelling of total number concentrations
121 (ToN) in the atmospheric urban environment. It is worth noting that about 99% of
122 ToN concentrations in the urban atmosphere are of sizes below 300 nm (Kumar et al.,
123 2009a) down to around 1.5–2 nm which is the size of stable nucleated particles
124 (Kulmala et al., 2007) . Therefore, the term ‘nanoparticle’ used in this work generally
125 refers to this size range (Kumar et al., 2010c). In what follows, the words
126 transformation and dynamics are used interchangeably as are the terms particle and
127 aerosol (according to the context).

128 **2. Key flow and mixing features in urban areas**

129 Wind flow and/or the mixing of the pollutants in that flow, through or above the
130 urban areas are not straightforward to describe. This is because of the complex
131 networks of streets and buildings, synoptic scale winds, surface heating and various
132 pollution sources such as moving traffic (Belcher, 2005), as seen in Fig. 1.
133 Incorporation of detailed turbulent mixing mechanisms (vehicle–induced turbulence,
134 road–induced turbulence and atmospheric boundary layer turbulence) improved

135 predictions of the spatial gradients of air pollutants near roadways (Wang and Zhang,
136 2009; Heist et al., 2009). Britter and Hanna (2003) proposed a simple approach to
137 describe urban scales; length scales such as street (L_s , less than ~100 to 200 m),
138 neighbourhood (L_N , up to 1 or 2 km), city (L_C , up to 10 or 20 km) and regional (L_R , up
139 to 100 or 200 km) scales. The smallest length scale is that of the vehicle wake (L_V)
140 where the mixing and dilution of pollutants occurs faster than at any other scale
141 (Baker, 2001; Carpentieri et al., 2010). Knowledge of both the flow and mixing at
142 various urban scales is essential for dispersion modelling of nanoparticles. The
143 following sections briefly explain these characteristics using an *inside–out* advection
144 approach. A summary of the key flow and mixing features at these urban scales is
145 given in Table 1.

146 **2.1 Vehicle wake**

147 For instance, a parcel of exhaust emission, containing pre–existing particles and
148 various precursor gases for condensation and new particle formation exits the tail
149 pipe. The vehicle wake is the first spatial scale where the emitted nanoparticles will
150 disperse into the ambient environment. The extent of any transformation of particles
151 depends on the flow characteristics and the turbulent mixing that govern the dilution,
152 and the background concentrations (Carpentieri et al., 2010). The vehicle wake
153 consists of two regions: (i) the near wake which is normally considered to be up to a
154 distance of about 10–15 times the vehicle height, and (ii) the far or main wake which
155 is a region beyond the near wake (Hucho, 1987). Number and size distributions of
156 nanoparticles change rapidly in the near wake due to the influences of various
157 transformation processes that are encouraged by the rapid turbulent mixing and
158 dilution (Kumar et al., 2009c; Solazzo et al., 2007). In the diluting and cooling
159 exhaust new particles form by homogeneous nucleation and immediately grow by
160 condensation of condensable vapours. Also, the high number concentration of newly
161 formed particles results in immediate coagulation of many of these particles,
162 transforming the particle size distribution. According to the on–road measurements by
163 Rönkkö et al. (2007), the nucleation mode was already formed after 0.7 s residence
164 time in the atmosphere. Many modellers use these size distributions as initial emission
165 size distributions. Thereafter in the far wake region, the rate of evolution is much
166 slower because vehicle–produced turbulence decays with the increasing distance from
167 the tailpipe and mixing is mainly dominated by atmospheric turbulence (Baker, 2001;
168 Eskridge and Hunt, 1979).

169 **2.2 Street canyons**

170 The emitted parcel of exhaust is further spread within the street canyon. This
171 spread is of particular interest because it occurs in traffic locations where people daily
172 spend relevant time, and where regulatory monitoring stations observe the air quality.
173 Direction of the flow is controlled by numerous factors: (i) geometry and aspect ratio
174 (average building height, H , to width, W , ratio) that classify them into regular, deep,
175 avenue, symmetric or non–symmetric canyons; Vardoulakis et al., 2003), (ii) urban
176 roughness elements within the canyon (trees, balconies, slanted roofs, etc.; Gayev and
177 Savory, 1999), (iii) street orientation (Hoydysh and Dabberdt, 1998; Vardoulakis et
178 al., 2003), and (iv) the synoptic wind conditions (Britter and Hanna, 2003).
179 Depending on the above–roof wind speed (U_r ; also called synoptic wind or free–
180 stream velocity), the flow can be: (i) neutral when $U_r < 1.5 \text{ m s}^{-1}$ and atmospheric
181 stability is neutral, (ii) perpendicular or near–perpendicular when $U_r > 1.5 \text{ m s}^{-1}$
182 blowing at an angle of more than 30° to the street axis, and (iii) parallel or near–

183 parallel when $U_r > 1.5 \text{ m s}^{-1}$ blowing from all other directions (Vardoulakis et al.,
184 2003). In case of regular street canyons (i.e. $H/W \approx 1$), the typical recirculating
185 velocities are $\approx 0.33\text{--}0.50 U_r$ and the turbulence levels are $\approx 0.10 U_r$ (Britter and
186 Hanna, 2003).

187 The *mixing* of the parcel within a canyon will depend on the ventilation flux of air
188 from the street canyon (Barlow et al., 2004; Caton et al., 2003), turbulence produced
189 by the wind (De Paul and Sheih, 1986), traffic (Solazzo et al., 2007, 2008) and
190 atmospheric instability (Xie et al., 2005). The shape and strength of the wind vortices
191 might also be affected by the atmospheric stability and other thermal effects induced
192 by the differential heating of the walls and/or the bottom of the canyon (Kim and
193 Baik, 2001; Sini et al., 1996). Wind- and traffic-produced turbulences (hereafter
194 referred as WPT and TPT, respectively) are generally considered to be the main
195 mixing mechanisms at this scale. During calm wind conditions (e.g. when U_r is below
196 about 1.5 m s^{-1}), the mixing of the parcel will be dominated by the TPT and
197 atmospheric stability conditions while the WPT will dominate the mixing during
198 larger wind speeds (De Paul and Sheih, 1986; Di Sabatino et al., 2003; Kastner-Klein
199 et al., 2003; Solazzo et al., 2007). The magnitude of mechanical mixing increases with
200 the increase in wind speed and surface roughness. Solar radiation heating the building
201 walls in a street canyon might generate upward buoyancy forces (Kim and Baik,
202 2001). However, laboratory, computational and field studies show only a small effect,
203 which is unlikely to be operationally important in most scenarios because the
204 physical width of the free convective boundary layer on the heated wall is small
205 compared with the scale of the mechanically driven motion (Kovar-Panskus et al.,
206 2002; Louka et al., 2002).

207 **2.3 Neighbourhood scale**

208 After the street scale, the parcel of exhaust can be assumed to be advected in the
209 neighbourhood through a network of streets, over and around several buildings (see
210 Table 1). The flow at this scale is more complex than in street canyons. This is due to
211 the interactions of the flow around several buildings and streets (Belcher, 2005).
212 There are two main characteristics: (i) the flow is assumed to have a long fetch over a
213 statistically homogeneous surface, and some quasi-equilibrium flow is established,
214 and (ii) the flow is assumed to have developed as a result of a change from one to
215 another region (Smits and Wood, 1985). Besides the factors playing a role in street
216 scale mixing, the neighbourhood scale is further affected by turbulence generated
217 from the interaction of flows coming from several sets of buildings and streets.
218 Detailed information on this scale can be seen elsewhere (Belcher, 2005; Britter et al.,
219 2002; Britter and Hanna, 2003; Coceal and Belcher, 2005; Grimmond and Oke, 1999;
220 Louka et al., 2000).

221 **2.4 City scale**

222 Further, the advection of a polluted air parcel can be extended to *city scale* (see
223 Table 1). This scale is composed of several neighbourhoods, and generally represents
224 the diameter of an urban area. This area can be distinguished from its surroundings by
225 its relatively large obstacles (buildings and other structures), the infusion of heat,
226 moisture from anthropogenic activities, the large heat storage capacity of concrete and
227 other building materials, and open spaces such as car parks. The city scale can include
228 variations in urban building types and spacing, and primarily concerns the
229 atmospheric boundary layer (ABL) above the average building height (H). To

230 characterise the ABL, which is almost always turbulent having a logarithmic wind
231 profile (Raupach et al., 1980; Rotach, 1993a, 1993b), it is important to comprehend
232 the complex flows and turbulent mixing processes at this scale (Fig. 1). The ABL
233 consists of three major sub-layers: (i) the urban canopy sub-layer where the flow at a
234 specific point is directly affected by local obstacles, (ii) the roughness sub-layer
235 where the flow is still adjusting to the effects of many obstacles, and (iii) the inertial
236 sub-layer where the boundary layer has adapted to the integrated effect of the
237 underlying urban surface (Britter and Hanna, 2003). The roughness sub-layer can
238 extend up to $\approx 2H$. It is generally assumed that a pollutant plume can extend vertically
239 up to $\approx 2H$ over the surface layer and that there is no need to account for the specific
240 effects around individual buildings. Consequently, pollutant concentration fields can
241 be determined by using standard approaches that apply to a general ABL (Di
242 Sabatino, 2005). The mixing of pollutants within the city is greatly influenced by the
243 complex orography (i.e. surface roughness) of the city and the TPT.

244 **2.5 Road tunnels**

245 The flow and mixing characteristics in road tunnels are entirely different than
246 other urban scales, and hence affect the transformation of nanoparticles diversely (see
247 Section 4). Unlike other urban scales, the factors governing the flow inside the tunnels
248 include vertical and horizontal aspirators transporting ‘clean’ air from the outside and
249 pushing it into the tunnel (called as ventilation speed), exhaust fans for discharging
250 the ‘dirty’ air outside the tunnel and the movement of the vehicles taking the air in
251 longitudinal direction out of the tunnel with their wakes (Bellasio, 1997; Cheng et al.,
252 2010; El-Fadel and Hashisho, 2001). The main flow inside the tunnel is induced by
253 the piston effect of the moving vehicles (Bari and Naser, 2010). The effect of
254 atmospheric turbulence (WPT and TCT) and the meteorological conditions (synoptic
255 wind speed and direction) on flow and mixing is insignificant compared with the TPT
256 during normal operational conditions. The flow is generally turbulent and the mixing
257 is intense within the tunnels due to the effect of the TPT in a confined environment
258 along with the buoyancy effects generated by the intake of ‘clean’ air and discharge of
259 ‘dirty’ air.

260 **3. Overview of dispersion models**

261 Several simple to complex models addressing dispersion of gaseous pollutants
262 and particulate matter (on a mass basis) at different urban scales are currently
263 available. These may include simple box models, Lagrangian or Eulerian models,
264 Gaussian models, and computational fluid dynamics (CFD) based models. This
265 section provides a brief overview of studies covering dispersion models but does not
266 go into the details of individual models. However, a brief discussion on the challenges
267 associated with the adaptation of gaseous dispersion models to nanoparticle
268 predictions on a number basis is presented.

269
270 Numerous studies in the past have covered dispersion models that address wind flow
271 and pollutant dispersions at vehicle wake, roadside locations, intersections, street
272 canyons, neighbourhood and city scales. A recent review by Seigneur (2009) mostly
273 focused on measurement techniques and ambient measurements of the physical and
274 chemical characteristics of ultrafine particles, besides synthesising some model
275 studies on the evolution of particles in vehicle exhaust plumes. Carpentieri et al.
276 (2010) reviewed various models and techniques used for the dispersion of
277 nanoparticles in the vehicle wake. Milionis and Davies (1994) analysed theoretical

278 aspects, advantages and disadvantages of regression and stochastic models for air
279 pollution studies Sharma and Khare (2001) reviewed commonly used analytical
280 models for the dispersion of vehicle exhaust emissions near roadways, intersections
281 and in street canyons. Later, Sharma et al. (2004) reviewed the philosophy and basic
282 features of commonly used highway dispersion models, together with statistical
283 analysis tools to evaluate the performance of these models. Gokhale and Khare (2004)
284 reviewed various deterministic, stochastic and hybrid (the combination of the former
285 two) vehicular exhaust emission models for traffic intersections and urban roadways.
286 Vardoulakis et al. (2003) presented a comprehensive review on dispersion models for
287 computing wind flows and transport of gaseous and particulate pollutants in street
288 canyons. The same group also reviewed sensitivity and uncertainty involved in street
289 scale dispersion models (Vardoulakis et al., 2002). Likewise, Li et al (2006) discussed
290 the various CFD modelling approaches for determining wind flow and pollutant
291 transfer within the street canyons. Holmes and Morawska (2006) reviewed several
292 simple and complex models covering a wide range of urban scales for the dispersion
293 of particulate matter. A recent study by Holmes et al. (2009) presented a summary
294 discussion of the activities, findings and recommendations of the US EPA funded
295 National Research Councils Committee on Regulatory Environmental Models for
296 assessing practice, pitfalls and prospects of various computational models used for
297 regulatory purposes. A comprehensive list of various dispersion models can be found
298 on Model Documentation System of European Topic Centre on Air and Climate
299 Change (MDS, 2010). Furthermore, a recent COST Action exercise presents various
300 model evaluation and quality assurance case studies (COST732, 2005-2009, 2010).

301 There are currently very few models which are especially designed to predict particle
302 number concentrations by taking into account the particle dynamics. A summary of
303 these models is presented in Table 2. Several models (Holmes and Morawska, 2006)
304 state that they include ‘aerosol dynamics’ but these generally predict various fractions
305 of particulate matter on a mass basis, not on a number basis. Theoretically, any
306 gaseous dispersion model should be able to predict number concentrations of inert
307 particles but this is usually not the case at all urban scales (see Table 2). Chemical and
308 physical processes associated with atmospheric particles show a non-linear
309 dependency on their sizes that varies over a broad range. Moreover, the effects of
310 these processes also differ at different urban scales. As discussed in Section 2,
311 complex flow and mixing due to intricate networks of streets and buildings, synoptic
312 scale winds, surface heating and various pollution sources such as moving traffic in
313 urban areas makes prediction of nanoparticle number and size distributions even more
314 challenging (Britter and Hanna, 2003). Nevertheless, gaseous dispersion models can
315 still be modified by integrating the particle dynamics module in them, since the
316 fundamentals for flow and pollutant dispersion predictions in a particular urban
317 setting remains the same. In this case, the most challenging task is to identify the role
318 of sinks and transformation processes and their appropriate treatment at various urban
319 scales (see Section 4). If mitigation policies for nanoparticles on a number basis are
320 adopted in the future, performance evaluation of such modified, new or existing
321 models against measured data in different operational conditions will be required.

322 **4. Relevance of particle dynamics in dispersion modelling**

323 In the beginning of this chapter we give a brief overview of the various
324 transformation processes acting on the particle number concentrations. A detailed
325 description and mathematical formulation of the different processes can not be given

326 here and is treated in several textbooks (e.g. Jacobson 2005; Seinfeld and Pandis,
327 1998; Hinds, 1999). Table 3 summarises the importance of transformation process at
328 different urban scales and their impacts on total number (and volume) concentrations.
329 Such information is essential since an inadequate treatment of these processes in
330 dispersion modelling may result in uncertainties in the predictions of nanoparticles
331 (see Section 5). Therefore, the effect of various processes at each urban scale is
332 explained separately. Only the processes which are shown as important in Table 3 are
333 included in discussions presented in Sections 4.2–4.5. In the final section 4.6 of this
334 chapter, a few examples for studies comparing several dispersion models for
335 nanoparticles are presented.

336 **4.1 Main underlining principles behind transformation and removal** 337 **processes**

338 *Emission* from the traffic source contributes to a broad number and size
339 distributions which generally have three distinct modes: nucleation, Aitken and
340 accumulation, and coarse (Kumar et al., 2010c). Each mode has its distinct
341 characteristics and changes both temporally and spatially due to the influence of
342 various processes. *Dilution* is a key process that supersedes and/or induces other
343 processes to act and alter the number and size distributions. Modelling studies agree
344 that both dilution and emissions need to be modelled in great detail before particle
345 dynamics are considered at all urban scales (Gidhagen et al. 2004a; Jacobson and
346 Seinfeld, 2004; Ketzel and Berkowicz, 2004).

347 *Homogeneous nucleation* forms new particles (initial size around 1.5–2 nm) through
348 gas-to-particle conversion (Kulmala et al., 2004; Wehner and Wiedensohler, 2003).
349 This occurs as a regional event in preferably clean air masses (not discussed in this
350 paper) and due to rapid dilution near the pollution sources. Nucleation and
351 condensation of sulphuric-acid and semi-volatile organic substances are responsible
352 for the formation of new liquid particles in vehicle exhaust during the first
353 milliseconds of dilution (Kittelson, 1998; Shi et al., 1999). This process exhibits
354 varying effects at different urban scales (Table 3) that needs to be modelled
355 appropriately. Since nucleation is happening directly after the exhaust is released into
356 the ambient air and very likely not later in the dilution process, it is possible and often
357 necessary to regard nucleation as part of the emissions and the corresponding
358 ‘effective’ vehicle emission factor for particle numbers. Often these ‘effective’
359 vehicle emission factors are observed to be dependent on ambient temperature (with
360 higher values at lower temperatures) (Olivares et al., 2007) and on sulphur content in
361 the fuel (higher values at higher sulphur content) (Wählén, 2009). Arnold et al. (2006)
362 measured gas-phase sulphuric acid concentration in the exhaust under some driving
363 conditions. Their results indicate that number concentration of nucleation mode
364 particles increased as an increasing sulphuric acid concentration. These dependencies
365 give a strong indication that nucleation plays a major role in the emission process. On
366 the other hand, some measurements indicate that the exhaust includes nucleation
367 mode particles that have a nonvolatile core (for example, oxidized metals or pyrolysed
368 hydrocarbons) formed before the dilution process (e.g. Sakurai et al, 2003; Rönkkö et
369 al., 2007). These core particles grow by condensation of semi-volatile material,
370 mainly hydrocarbons, during dilution and cooling.

371 *Coagulation* is the process in which particles collide due to their random (Brownian)
372 motion and coalesce to form larger particles and agglomerates which are made up of
373 several particles. Brownian motion is enhanced by Van der Waals forces, viscous
374 forces, and fractal geometry of aggregates. Van der Waals forces are the result of the
375 formation of momentary dipoles in uncharged, nonpolar molecules (Seinfeld and
376 Pandis, 2006). They enhance the coagulation rate of small particles whereas they are
377 weakest in the continuum regime (Jacobson and Seinfeld, 2004). For small particles,
378 fractal geometry enhances the coagulation kernel with increasing size of the colliding
379 particle. Coagulation is especially efficient between particles of different sizes, with
380 smaller particles having high mobility and larger particles providing a large cross-
381 section. The coagulation process reduces the number of (mainly) the smaller particles
382 while preserving the total mass. However, coagulation modifies the particle number
383 size distribution, and internally mixes particles of different original composition over
384 the population (Jacobson, 2002). Neglecting coagulation in models will over-predict
385 the nanoparticle number concentration even in the cases if particles below 10 nm are
386 not included in the simulations. When this process takes place between solid particles,
387 the process is sometimes called agglomeration and the resulting particle clusters are
388 known as agglomerates (Hinds, 1999).

389 *Condensation* is a diffusion-limited mass transfer process between the gas phase and
390 the particle phase governed by the higher vapour pressure of condensable species in
391 the air surrounding the particles. Condensation causes an increase in the volume of
392 particles but does not change number concentrations. Condensation and nucleation are
393 often competing processes since both involve condensable gas species that either can
394 condense on pre-existing particles or form new nucleating particles (e.g. Jacobson et
395 al., 2002; Pirjola et al., 2004; Kulmala et al., 2004 and references therein). Smaller
396 concentrations of pre-existing particles favour both the production of new particles
397 and their growth to detectable sizes (Kulmala et al., 2004). Conversely, high
398 concentrations of pre-existing particles promote the condensation of the semi-volatile
399 vapours and disfavour both the growth of fresh nuclei and their survival from high
400 coagulation scavenging (Kerminen et al., 2004).

401 *Evaporation* is the reverse process compared to condensation, which reduces the
402 volume concentration of particles. It occurs when molecules on a particle surface
403 change to the gas phase and diffuse away from the surface driven by the lower vapour
404 pressure in the air (Jacobson, 2005). Ultrafine particles evaporate faster than coarse
405 particles due to the Kelvin effect (Hinds, 1999; Fushimi et al., 2008), and lose more
406 volume because of their volatile nature (Kittelson et al., 2004). Semi-volatile organics
407 evaporate almost immediately from liquid particles that are composed of unburned
408 fuel, unburned lubricating oil and sulphate, and form near the tailpipe by nucleation
409 and condensation during initial dilution and cooling (Jacobson et al., 2005). It is not
410 just the heating which evaporates the volatile material from the ultrafine particles, a
411 low carbon number (high volatility) of organic compounds (Sakurai et al., 2003) and
412 dilution of volatile gases can also cause the particles in the ultrafine size range to
413 shrink by evaporation (Zhang et al., 2004). Kuhn et al. (2005) studied the volatility of
414 both outdoor and indoor particles. They heated the particles to 60°C and did not
415 observe significant losses in number or volume concentrations but these particles
416 shrank to approximately half of their original size at 130°C where they attained their
417 non-volatile core. Evaporation seems to be important during periods of high ambient
418 temperature and for the spatial scales dominated by high dilution (e.g. wake regions;

419 see Section 4) and fresh emissions (e.g. roadside). It should also be noted that partial
420 evaporation increases the rate of coagulation by increasing the diffusion coefficient of
421 the remaining particles (Jacobson et al., 2005).

422 *Dry deposition* removes particles through deposition to air–surface interfaces
423 (Seinfeld and Pandis, 2006). This process is mainly driven by Brownian diffusion and
424 inertial impaction. The former is more effective for nucleation mode particles due to
425 their larger diffusion coefficient and the latter is only important for particles larger
426 than 100 nm in turbulent flow conditions (Lee and Gieseke, 1994). Dry deposition is
427 therefore an important process to consider in dispersion modelling at all scales. A
428 review of various size resolved particle dry deposition schemes for air quality and
429 climate models can be found in Petroff and Zhang (2010).

430 *Wet deposition* removes particles by precipitation (Laakso et al., 2003). This can
431 occur by two processes: nucleation scavenging (rainout) and aerosol–hydrometeor
432 coagulation (washout). Washout is due to coagulation of precipitation hydrometeors
433 with interstitial and below–cloud aerosols whereas rainout is due to the removal of
434 precipitation and incorporated aerosols (Jacobson, 2003). Based on the model
435 simulations, Jacobson (2003) concluded that washout appears to play a substantial
436 role in controlling aerosol number globally. On the other hand, rainout is an ‘episodic’
437 process which is more relevant to the removal of coarse particles (aerosol mass) but
438 does not show countable effects on the removal of ultrafine particles (<100 nm). For
439 example, Andronache (2005) reported that ultrafine particles formed in the ABL (see
440 Fig. 1) by the nucleation process need to grow to a diameter of ~100 nm to become
441 activated as cloud droplets. By considering a typical growth rate of about 5 nm h⁻¹
442 (Kulmala et al., 2004), the time required to reach to about 100 nm is approximately 2–
443 3 days. If precipitation occurs, most ultrafine particles are too small to become cloud
444 droplets, and only a few particles are removed by this scavenging process
445 (Andronache, 2005).

446 **4.2 Transformation processes in the vehicle wake**

447 The flow and dispersion in the vehicle wake has been discussed in Section 2.1.
448 The intensity of turbulence and dilution in wake regions can be described by the
449 dilution ratios, being the ratio of the volume of a polluted air parcel after dilution to
450 original volume before. For instance, Zhang and Wexler (2004) reported that dilution
451 ratio can reach up to 1000:1 in 1–3 s after the release of emissions. Kittelson (1998)
452 found about the same dilution ratio occurring in 1–2 s behind the tailpipe during their
453 field study. These numbers can be related to the near wake region though these studies
454 did not distinguish wake regions explicitly. These observations also indicate that the
455 time scales for evolution in the near–wake are substantially smaller, and hence
456 capturing them *experimentally* is highly challenging due to a limited sampling
457 frequency of available particle spectrometers (Kumar et al., 2010c). Therefore,
458 computational studies could be useful if used to gain detailed insight into near–wake
459 processes (Albriet et al., 2010; Chan et al., 2010). Conversely, the case for the far–
460 wake region is relatively less complicated where the particle processes may last up to
461 10’s of seconds, depending on the local geometry of urban settings and the
462 atmospheric conditions (Kumar et al., 2009c; Zhang and Wexler, 2004).

463 Irrespective of any wake region, a common finding from the studies are that the
464 dilution is the most important parameter (Jacobson and Seinfeld, 2004; Uhrner et al.,

465 2007; Zhang and Wexler, 2004; Pohjola et al., 2003; 2007) and should be considered
466 appropriately in dispersion models. This is followed by the nucleation, condensation
467 and deposition of nanoparticles. On a short time scale coagulation of particles above
468 10 nm is too slow to substantially affect the number concentrations. Summary of their
469 importance and effect on ToN concentrations are presented in Table 3 while below
470 some references from the literature are discussed.

471 **4.2.1 Role of transformation and removal processes in near- and far-wake**

472 Kumar et al. (2009c) measured number and size distributions in the wake of a
473 moving vehicle. They found that dilution was so quick in the near-wake of a moving
474 vehicle that the competing effects of the transformation processes were nearly over
475 within 1 s after emission. Further extension of these experiments included both
476 ground-fixed and on-board measurements of particles in the 5–560 nm size range in
477 the wake of a moving diesel car running at 4 different speeds (Carpentieri and Kumar,
478 2011). Up to four sub-stages of particle evolution were observed during various
479 experimental runs. Each sub-stage showed distinct evolution patterns of particle size
480 distributions. In line with the previous results, dilution was found to be a dominant
481 process throughout all the evolution stages. Dilution generally follows the “power
482 law” (i.e. increasing with distance (x) in the vehicle wake) depending on traffic type
483 and conditions. Approximate maximum value of dilution profile, $D(x)$, immediately
484 after the emissions can be estimated using the following equations: $17.6x^{1.3}$ (Zhang
485 and Wexler, 2004) or $7.01x^{0.955}$ (Kittelson et al., 1988). Zhang and Wexler (2004)
486 modelled the exhaust emissions coming from different type of engines and examined
487 the effect of dilution, nucleation, condensation and coagulation processes on the
488 different size distributions between the tailpipe and road. Uhrner et al. (2007)
489 performed a detailed CFD calculation of particle formation by nucleation and
490 dispersion directly in the vehicle wake and compared them to on-road measurements.
491 Both studies concluded that new particle formation through sulphuric-acid triggered
492 nucleation and growth of these particles is the dominant particle production
493 mechanism which depends on the amount of condensable materials remaining in the
494 gas phase at the exit of tailpipe. Ketzler et al. (2007) also observed that particle number
495 emissions can double when temperature decreases from +20 to +5 °C due to particle
496 formation in the immediate exhaust plume. Because the nucleation process depends
497 on ambient temperature, it might be responsible for the observed temperature
498 dependence of the emission factors. This is then followed by the condensation of
499 organic compounds, resulting in the rapid growth of nucleation mode particles and
500 relatively slow growth of accumulation mode particles.

501

502 Pohjola et al. (2003) simulated the time evolution of Aitken and accumulation mode
503 particles emitted by a light duty diesel vehicle in the wake region for 25 s. They found
504 that condensation of an insoluble organic vapour was important if the concentration of
505 the condensable vapour exceeds a value of 10^{10} or 10^{11} molecules cm^{-3} for Aitken and
506 accumulation mode particles, respectively, and that the effect of coagulation was
507 substantial only, if dilution was neglected. Likewise, a recent study by Chan et al.
508 (2010) computationally simulated these processes in the vehicle wake. They
509 concluded that nucleation and coagulation processes were nearly complete within the
510 near-wake regions (i.e. within 0.25–0.5 m, and 4 m, respectively) behind the
511 vehicular exhaust tailpipe, and dilution then spreads the particles which are carried by
512 advection from the near wake to the far wake. In the far-wake region, particles can

513 still grow by condensation but the growth rates decrease with distance away from the
514 tailpipe due to decreasing dilution factor and concentrations of condensable species.
515 Time scales for coagulation are considerably larger compared with dilution (Fig. 3)
516 meaning that under many conditions coagulation is slow enough, compared with
517 dilution, to reduce the ToN concentrations. Based on time scale analysis of Brownian
518 coagulation for a particle size distribution measured on highway, Zhang and Wexler
519 (2004) stated that coagulation plays minor role in the far wake region; however,
520 coagulation will have some effect on particles below 10 nm or under slow dilution
521 conditions. Likewise, Kerminen et al (2007) showed that the slow dilution due to
522 inefficient mixing gives time for many other aerosol processes, such as self- and
523 inter-modal coagulation as well as condensation and evaporation, to become
524 important. Jacobson and Seinfeld (2004) found that dilution is more important than
525 coagulation at reducing the ToN concentrations near the source of emission, but the
526 relative importance of dilution versus coagulation varies with concentration. In any
527 case, coagulation cannot be ignored in the models. Jacobson et al. (2005) found that
528 treating the additional process of evaporation of low-molecular-weight organic
529 vapours from small (<15 nm) liquid particles enhanced their coagulation rates
530 allowing for the full particle evolution to be accounted for.

531 Potentially relevant removal mechanisms of nanoparticles in the near- and far-wake
532 region are the dry and wet deposition. As discussed in Section 4.1, nucleation
533 scavenging (rainout) can be ignored whereas washout is important removal
534 mechanism at least for city scale modelling. Dry deposition is an important process
535 for both wake regions. Dry deposition can substantially remove particles at the air-
536 road interface (Gidhagen et al., 2004a; Gidhagen et al., 2004b). Fig. 2 shows the size
537 dependent deposition speed using the resistance model (aerodynamic resistance,
538 molecular diffusion, and chemical, biological and physical interactions) suggested by
539 Seinfeld and Pandis (2006) and an alternative description based on several field
540 studies by Shack Jr et al. (1985).

541 **4.3 Street canyons**

542 There is a consensus in the literature that removal processes such as dilution and
543 dry deposition should be considered at street scale modelling (Gidhagen et al., 2004a;
544 Ketzal et al., 2007). Evidence of dilution dominating over other processes is evident
545 from the studies showing high correlation between particle number concentrations and
546 NO_x which is generally inert at street scale (Jacobson and Seinfeld, 2004; Ketzal et
547 al., 2007). Similarly, deposition onto the road surface and/or walls in the street
548 canyons is strongly influenced by the traffic movement. This can reduce the total
549 number concentrations by about 10–20% in a street canyon (Gidhagen et al., 2004a;
550 Ketzal et al., 2007).

551 There are two contentions about the role of nucleation, coagulation and condensation
552 at street scale. One that favours their inclusion in dispersion models and the others
553 that does not. Literature (e.g. Gidhagen et al., 2004a; Ketzal and Berkowicz, 2004)
554 shows evidence in support of both these contentions but the underlining principles, as
555 discussed in Section 4.1, remain the same that relevance of these processes may vary
556 at different locations depending on the concentration of the exhaust emissions, the
557 background concentrations (pre-existing particles) and meteorological conditions
558 (Charron and Harrison, 2003; Wehner et al., 2002). Moreover, competing influences
559 of the various processes might cancel each other and in total not affect the net particle

560 number concentrations notably (Kumar et al., 2009a; Kumar et al., 2008c). For
561 example, Vignati et al. (1999) applied a Brownian coagulation–dilution model to a
562 plume emitted from a diesel engine into the street air. The emitted particle size
563 distribution possessed one or two modes covering particles in the size range of 0.002–
564 10 μm . They found that due to rapid dilution only very small particles ($<0.002 \mu\text{m}$)
565 have a coagulation time scale which is comparable with typical residence times of
566 pollutants in a street. They also found that condensation does not lead to any
567 substantial transformation of the particle size distributions as water vapour
568 condensation on freshly emitted diesel particles led to only a marginal increase in
569 particle size.

570 One method of determining the relative importance of various processes is a *time*
571 *scale analysis*, as seen in Fig. 3 for the processes dilution, deposition and coagulations
572 at different urban scales (Ketzel and Berkowicz, 2004). The process with the smallest
573 time scale at a specific spatial scale (exhaust plume, kerbside etc.) is the fastest and
574 most relevant to include in numerical modelling. Dilution is by far the most relevant
575 process at all scales, except for the road tunnel, where dilution is slowed down by the
576 confined environment and acts at similar time scale as deposition and coagulation. At
577 street scale deposition occurs about 10 times slower (i.e. larger time scale) than
578 dilution. Separately, time scales were estimated for a street canyon in Cambridge, UK
579 (Kumar et al., 2008c). The deduced time scales were of the order of 40s for dilution,
580 30 to 130s for dry deposition on the road surface, and 600 to 2600s for the dry
581 deposition on the street walls, about 10^5 s for coagulation, and about 10^4 – 10^5 for
582 condensation for extreme growth rates at 1 and 20 nm h^{-1} , respectively (Kumar et al.,
583 2008c). Comparison of these estimated time scales shows that dilution is quick and it
584 does not allow other processes (except for dry deposition on the road surface) to alter
585 the size distributions.

586 In the following we present further observations supporting the view that particle
587 dynamics could be ignored at street scale, especially when either sub–10 nm particles
588 or Van der Waals forces and the effects of fractal geometry on such forces are not
589 considered. As a part of a recent study (Kumar et al., 2009c), the time scales of
590 particle evolution in the wake of a moving vehicle (~ 1 s) were compared with the time
591 scales for these particles to reach the kerb side in a street canyons (~ 45 s). These
592 observations led to the hypothesis that ‘the competing influences of transformation
593 processes were nearly over by the time these particles are measured at the road side
594 and ToN can then be assumed to be conserved’. Consistent with this were the
595 observations found during the pseudo–simultaneous measurements of particle number
596 and size distributions where measurements were made at 4 different heights (1 m,
597 2.25 m, 4.62 m and 7.37 m) of an 11.75 m high regular street canyon (Kumar et al.,
598 2008c). Results indicated that number and size distributions were similar in shape,
599 peaking at about 13.3 nm and 86.6 nm and shifting upwards and downwards at
600 different heights due to the combined effect of dilution and vertical concentration
601 gradient in the canyon (see Fig. 4). Moreover, there was negligible shift in geometric
602 mean diameters of number and size distributions in both modes at each height (i.e.
603 16.4 ± 0.9 nm for particles in the 10–30 nm range and 64.7 ± 5.1 nm for 30–300 nm
604 range). Similar results were reported by Ketzel and Berkowicz (2004), Gidhagen et al.
605 (2004a) and Pohjola et al. (2003, 2007) on the treatment of street level particle
606 dynamics in dispersion models.

607 **4.4 Neighbourhood and city scales**

608 There are contrasting conclusions on the role of coagulation under typical urban
609 ambient conditions. Few studies show coagulation is too slow to alter the particle size
610 distributions (Gidhagen et al., 2005; Zhang and Wexler, 2002) but others show
611 significant particle growth to the effect of coagulation in urban environments (Wehner
612 et al., 2002) or during episodic conditions (Gidhagen et al., 2003). City scale
613 modelling studies agree with the latter, showing a countable effect of coagulation on
614 number concentrations (Ketznel and Berkowicz, 2005).

615 Condensation and evaporation do not change the total number concentrations but will
616 alter the size distributions and particle volume. A number of nucleation mechanisms
617 such as the binary water–sulphuric acid nucleation, ternary water–sulphuric acid–
618 ammonia nucleation, ion–induced nucleation or photochemically induced nucleation
619 play a role in the formation of new particles (Kulmala et al., 2004). For urban
620 locations, growth rates are generally between 1 and 10 nm⁻¹ and the new particle
621 formation rate is about 100 # cm⁻³ s⁻¹ (Kulmala et al., 2004), indicating a notable
622 effect on ToN concentrations. Therefore, most of these processes are taken into
623 account in various urban scale models (e.g. MAT, MATCH) described in Table 2.
624 Differences between measurements and model calculations using MAT (with and
625 without particle processes) were estimated by Ketznel and Berkowicz (2005). They
626 reported that coagulation can remove 10% of the total number concentrations while
627 dry deposition can remove between 50–70% depending on the assumed value of
628 removal velocities. Model calculations using MATCH by Gidhagen et al. (2005)
629 reported losses, as compared with inert treatment, due to dry deposition up to 25%
630 under average meteorological conditions while these can be up to 50% during
631 episodes with low wind speeds and stable conditions. The overall ranges of change
632 including all processes compared with inert treatment can lie between 13 and 23% of
633 loss in ToN concentrations (Ketznel and Berkowicz, 2005).

634 **4.5 Road tunnels**

635 In a confined environment like a road tunnel, particles collide and merge with
636 each other due to an accumulation of particles with the increasing length of the tunnel
637 (Cheng et al., 2010). Thus, studies have identified coagulation and deposition as the
638 most important depletion processes (Gidhagen et al., 2003; Sturm et al., 2003). Both
639 processes show larger influence on smaller particles of less than about 30 nm. Model
640 calculations (MONO32 with the CFD code StarCD) by Gidhagen et al. (2003) showed
641 that combined losses of coagulation and dry deposition onto the tunnel walls, were
642 about 77% and 41% of the ToN concentrations for particles smaller than 10 nm and
643 between 10 and 29 nm, respectively. Due to the presence of precursor gases in high
644 concentrations and intense mixing due to traffic–produced turbulence, road tunnels
645 provide an ideal environment for the formation of nucleation mode particles.
646 However, coagulation is generally found to be fast enough to efficiently remove the
647 smallest particles (Cheng et al., 2010; Gidhagen et al., 2003; Ketznel and Berkowicz,
648 2004).

649 **4.6 Modelling case studies showing effects of transformation processes 650 on ToN concentrations and size distributions**

651 Two case studies using five different models are included in this section. The
652 first study shows the effect of various transformation processes on number and size
653 distributions of particles at city scale. The other study shows modelled ToN

654 concentrations (assuming the particles as inert tracer) and their comparison with the
655 measurements at street scale.

656 **4.6.1 Modelling of particle size distributions using MAT and AEROFOR** 657 **model**

658 This section presents a modelling case study that was based on data from the
659 Copenhagen area assuming prevailing westerly wind, using the models AEROFOR
660 and MAT (see Table 2 for model details). The processes included in the modelling are
661 emissions from a near ground source, dilution with background air, deposition,
662 Brownian coagulation and condensation (Ketznel and Berkowicz, 2005; Ketznel et al.,
663 2007). In this work, the size range of particles treated in the models is from 1 nm to 2
664 μm .

665 The simulation starts at time = 0 s assuming a background particle size distribution
666 measured at the station Lille Valby located west of Copenhagen, i.e. upwind for the
667 assumed case. The air mass is then transported over an urban traffic-related area
668 source with a constant wind speed. The evolution of the size distribution will be
669 followed by the two models for a certain simulation time, assuming a homogeneous
670 emission density of the area source having a typical size distribution for traffic
671 emitted particles. Model runs are performed with sensitivity analysis for specific
672 processes included or excluded in the simulations. The outputs of the both models are
673 shown in Fig. 5. There are two points to notice: (i) the comparison of results between
674 two models, and (ii) the effect of processes on number and size distributions. Note
675 that the case 'EmDi' represents the reference case considering the particles as inert
676 (i.e. a case without removal or aerodynamic processes). The cases added to EmDi is
677 condensation (+Con), coagulation (+Coa), deposition (+De), deposition and
678 coagulation (+DeCoa), deposition, coagulation and condensation (+DeCoaCon). For
679 the condensation process two different versions are considered that differ in the
680 concentration of the condensing vapour that corresponds to typical urban growth rates
681 of 1 nm/h (...Con1) and 6 nm/h (...Con2).

682 Considering the complexity of the modelled cases, results shown in Fig. 5 between
683 both models indicate a good agreement. Both models treat aerosol dynamics in a
684 similar way, except the dry deposition which has different parameterisation in
685 AEROFOR. Consequently, effect of dry deposition on the size distributions by the
686 AEROFOR is so small that we cannot distinguish the case EmDi (not shown in the
687 graphs) from the case EmDi+dep. This is also the reason why the curves for
688 EmDi+coa and EmDi+DeCoa overlap in Figs. 5b, d. Coagulation is less efficient in
689 reducing ToN concentrations at the start of the simulations, when concentrations are
690 lower as compared to the end of the simulations (Figs. 5a, b). Larger deviations
691 between the two models were observed for the simulations including treatment of
692 condensation (see Figs. 5c, d). This is expected since the chemical composition and
693 properties of the aerosol are different in the two models.

694 **4.6.2 Modelling of ToN concentrations using CFD, OSPM and a modified** 695 **Box model**

696 ToN concentrations in the 10–300 nm size range were modelled using a
697 simple modelling approach (modified Box model, including vertical variation), the
698 operational street pollution model (OSPM) and the CFD code FLUENT (Kumar et al.,
699 2009b). All models neglected the particle dynamics. CFD simulations were carried

700 out using a standard κ - ε turbulence closure scheme (κ is turbulent kinetic energy and
701 ε is dissipation rate of kinetic energy; Vardoulakis et al., 2011) in a simplified
702 geometry of our previously studied street canyon which has height (H) to width (W)
703 ratio of about unity (i.e. $H = W = 11.6$ m). ToN concentrations were measured
704 pseudo-simultaneously on the leeward side of the canyon at four different heights i.e.
705 $z = 1.00$ m, 2.25 m, 4.67 m and 7.37 m (Kumar et al., 2008c). These measurements
706 were made continuously using a differential mobility spectrometer (DMS500) in the
707 5 – 2500 nm size range at a sampling frequency of 0.5 Hz (Kumar et al., 2008a; Kumar
708 et al., 2008c). Measured ToN concentrations at different heights were compared with
709 the modelled concentrations from all three models (see Fig. 6 of Kumar et al., 2009b).
710 The values of correlation coefficients (R) for OSPM, CFD and modified Box model at
711 $z = 1.00$ m were 0.84 , 0.80 and 0.80 , at $z = 2.25$ m were 0.85 , 0.90 and 0.90 , at $z =$
712 4.67 m were 0.75 , 0.69 and 0.70 , and at $z = 7.37$ m were 0.74 , 0.69 and 0.71 ,
713 respectively. Each model showed good agreement with measurements with values of
714 R that ranged between 0.7 and 0.9 . The values of R were relatively larger for the
715 OSPM at all heights (except for $z = 2.25$ m) than for the Box and CFD models. The
716 OSPM consistently under-predicted the ToN concentrations while the other two
717 models over-predicted the concentrations in most cases. Furthermore, ToN
718 concentrations predicted by the Box and CFD models were generally in closer
719 agreement compared with the OSPM results. This could be because the OSPM
720 explicitly takes into account the turbulence created by the traffic (Vardoulakis et al.,
721 2007), which was not the case for other two models. Furthermore, differences
722 between the modelled results and measurements can be attributed to a large
723 uncertainty in the particle number emission factors (PNEF) as discussed in Section
724 5.2. Overall, the modelled and measured concentrations were found to agree within a
725 factor of two to three, which is a fairly good agreement for ToN concentrations. These
726 observations support to a certain extent the hypothesis presented in Section 4.3 that
727 the role of particle dynamics may be ignored for street scale modelling when particles
728 down to 1 nm size are not considered, although it can be argued that inclusion of
729 particle dynamics might have marginally improved the modelled results. Gidhagen et
730 al. (2004a) simulated the particle dynamics in a street canyon in Stockholm using the
731 combined results of MONO32 and CFD model StarCD (see Table 2 for details) and
732 found about 10 – 30% larger losses in ToN concentrations as compared with inert
733 treatment during low wind conditions. However, this effect would be much smaller
734 during average wind conditions due to the efficient ventilation of the canyon (Section
735 2) and less ToN concentrations. Moreover, this potential improvement in modelled
736 ToN concentrations would come at the cost of complex modelling and heavier input
737 information requirements.

738 **5. Uncertainties in dispersion modelling of nanoparticles**

739 Particle dispersion models suffer from the similar uncertainties associated with
740 the gaseous dispersion models in addition to the uncertainties related to the particle
741 dynamics. All models represent simplifications of various processes and such
742 simplifications can produce mainly two types of uncertainties, (i) structural, and (ii)
743 parametric, in addition to inherent uncertainties related to stochastic processes (e.g.
744 turbulence) in the atmosphere (Holmes et al., 2009; Vardoulakis et al., 2002).
745 Stochastic processes play an important role in the dispersion of nanoparticles, e.g.
746 atmospheric turbulence (see Section 2) leads to their dilution that in turn can change
747 the number and size distributions of nanoparticles, as described in Section 4.
748 However, stochastic fluctuations cannot be accurately modelled, although they are

749 approximated in semi-empirical and CFD models. The following two subsections
750 focus on the structural and parametric uncertainties associated with the dispersion
751 modelling of nanoparticles.

752 **5.1 Structural uncertainty**

753 Structural uncertainties are due to the fundamental representation of the
754 physical and chemical processes considered in the model structure. COST Action732
755 (2005-2009) suggest a method for inter-comparing the structural uncertainty of
756 gaseous dispersion models by comparing the modelled results with the observations.
757 These also apply for the particle dispersion models and include frequently used testing
758 parameters: (i) FB (fractional bias), (ii) FAC2 (fractions of predictions within a factor
759 of 2), (iii) NMSE (normalised mean square error), (iv) MG (Geometric mean), and (v)
760 VG (geometric variance). Inappropriate treatment of the sinks and transformation
761 processes at various urban scales in nanoparticle dispersion models is one
762 predominant reason for additional structural uncertainties than those in gaseous
763 dispersion models (see Section 4). However, the degree of this type of uncertainty will
764 vary at different urban scales depending on the relevance of particle transformation
765 processes. One way of reducing such type of uncertainty is by introducing more
766 physically realistic and computationally efficient algorithms for various relations and
767 nanoparticles (Vardoulakis et al., 2002). Uncertainty exists in some numerical
768 techniques (e.g. conservative versus non-conservative schemes) and particle size
769 distribution representations by moment methods (modal and monodisperse) and by
770 sectional methods.

771 **5.2 Parametric uncertainty**

772 Parametric uncertainty is due to the use of uncertain input values (e.g. wind
773 speed and direction, traffic volume, number emission factors) for model calculations.
774 This may be due to the lack of representative datasets (e.g. local meteorological data),
775 uncertainties in data (e.g. instrument calibration, unsteadiness in the measurement
776 conditions) or limited knowledge of key parameters (e.g. emission factors). For
777 example, Lohmeyer et al. (2002) reported that predictions of gaseous pollutants from
778 different models can vary up to a factor of four for identical situations, depending on
779 the quality of input information. However, such comparative studies are not currently
780 available for nanoparticle dispersion models, although they are essential for
781 improving dispersion models that can be used for developing mitigation policies.

782 It is recognised that the main source of parametric uncertainty in dispersion models
783 lies with the PNEFs (e.g. Holmes and Morawska, 2006). The PNEFs are directly
784 proportional to the predicted particle number concentrations, therefore any inaccuracy
785 in their estimation would directly lead to a similar degree of inaccuracy in the model
786 predictions. Number and size distributions of particles change rapidly after the
787 emissions exit the tailpipe due to rapid dilution similar to gaseous pollutants. However
788 unlike gaseous pollutants, the particle number concentration flux can not be conserved
789 due to secondary particle formation e.g. by dilution induced nucleation (Wehner et al.,
790 2009). Therefore, there are no standard databases available for routine use. Moreover,
791 studies on emissions from specific types of vehicles under controlled conditions (e.g.
792 constant speed or load) provide very limited information on the PNEFs for different
793 types of vehicles or a composite fleet of vehicles under real-world urban driving
794 conditions.

795 PNEF studies use several methods for their estimations. Most commonly used
796 methods involve (i) road side measurements of air pollutants and accounting for
797 dispersion by use of models, so-called 'inverse modelling technique' or by use other
798 pollutants with known emissions as NO_x or CO₂ so-called 'tracer method' (Corsmeier
799 et al., 2005; Gidhagen et al., 2004a; Gidhagen et al., 2004b; Gidhagen et al., 2003;
800 Gramotnev et al., 2003a; Gramotnev et al., 2004; Hueglin et al., 2006; Imhof et al.,
801 2005a; Imhof et al., 2005c; Jamriska and Morawska, 2001; Jones and Harrison, 2006;
802 Keogh et al., 2009; Ketzel et al., 2003; Kittelson et al., 2004; Kumar et al., 2008b;
803 Kumar et al., 2008c; Morawska et al., 2005; Rijkeboer et al., 2005; Zhang et al., 2005;
804 Zhu and Hinds, 2005), (ii) motorway tunnel measurements (Abu-Allaban et al., 2002;
805 Imhof et al., 2005b; Kirchstetter et al., 2002; Kristensson et al., 2004), (iii)
806 measurements directly through chassis dynamometer tests at the exit of tailpipe (Dahl
807 et al., 2006; Jayaratne et al., 2009; Morawska et al., 1998; Prati and Costagliola, 2008;
808 Ristovski et al., 2005; Ristovski et al., 2002; Ristovski et al., 2004), or (iv)
809 measurements in the exhaust plume of individual cars under real-world conditions by
810 remote sensing or so-called car-chasing (Hak et al., 2009; Vogt et al., 2003; Wehner
811 et al., 2009). While the first methods (i+ii) provide data for a mixture of many
812 vehicles (vehicle fleet) the latter methods (iii+iv) give results for a limited number of
813 individual cars. A comprehensive summary of numerous PNEF studies, categorised
814 by vehicle types, is presented in Table 4.

815 The chassis dynamometer method measures PNEFs close to the source. The other
816 methods, such as inverse modelling techniques, estimate PNEFs using ambient
817 concentrations close to the receptor but away from the source. The *source* and
818 *receptor* based PNEFs are different from each other because of the unequal treatment
819 of the transformation processes in dispersion models. Whether it is appropriate to
820 choose *source* specific PNEFs for modelling purposes as opposed to the receptor
821 specific PNEFs is highly debatable. Source based estimates of the PNEFs can be more
822 appropriate because these accurately represent the emission strength of a vehicle.
823 However, such measurements leave the transformation processes occurring between
824 the tailpipe and the receptor location to be accounted by the dispersion models which
825 have their own limitations in treating the particle dynamics. On the other hand,
826 receptor based estimates of the PNEFs are back-calculated from the roadside ambient
827 measurements which have already undergone natural transformation processes by the
828 time they reach the measurement site. These estimates are based on realistic
829 nanoparticle concentrations but may not represent the actual emission strength of a
830 vehicle or a traffic fleet since effects of transformation processes in inverse modelling
831 methods are generally ignored. Therefore adequate treatment of particle dynamics is
832 essential in nanoparticle dispersion models that are used for back-calculating PNEFs
833 (Wehner et al., 2009).

834 Other factors influencing the estimates of PNEFs include vehicle type, speed, load
835 and driving conditions, lower and upper cut-off values of the particle size range
836 considered, and sulphur content in the fuel. Typical driving conditions in urban
837 environments represent varying vehicle speed, with stop-start or acceleration-
838 deceleration conditions, leading to a considerable variability in particle emissions
839 from vehicles and uncertainty in PNEF estimates (Kittelson et al., 2004). Vehicle
840 speeds are generally expected to be less than 60 km h⁻¹ in typical driving conditions in
841 the urban areas. A closer inspection of the summary of several studies presented in

842 Table 4 indicates up to an order of magnitude difference in the PNEFs for a mixed
843 traffic fleet under near-identical conditions.

844 If we look at the different vehicle types independently (Table 4), it can be seen that
845 emissions of petrol vehicles are much more engine load and vehicle speed dependent
846 compared with diesel vehicles (Kittelson et al., 2004). However, the PNEFs from light
847 duty diesel vehicles (especially cars and buses) are expected to be relatively consistent
848 (i.e. within a factor of 3) compared with heavy duty vehicles that can have up to an
849 order of magnitude larger than light duty petrol or diesel vehicles (Imhof et al., 2005c;
850 Prati and Costagliola, 2008). These observations reflect the large uncertainty in
851 PNEFs meaning that modelled results are likely to be affected to a similar degree
852 irrespective of the accuracy of the dispersion model.

853 Sulphur content of the fuel also plays a major role in the formation of nanoparticles
854 and consequently influences the PNEFs. For example, the sulphur content in Danish
855 fuels was reduced twice from 500 ppm to 50 ppm in 2000 and to 10 ppm in 2005; in
856 both cases changes in the emitted size distribution of particles were observed. Studies
857 by Wåhlin et al. (2001) and Wåhlin (2009) indicate about 27% reduction in average
858 particle number concentration from the period 2002–2004 to the period 2005–2007
859 during their kerbside study at a busy street in Copenhagen. Most of these reductions
860 were in the ultrafine size range and more particularly in particles below 30 nm.
861 Similar observations were found by Ristovski et al. (2006) in their chassis
862 dynamometer study on low and ultra low sulphur buses in Brisbane, Australia.

863 **6. Conclusions and future research challenges**

864 This article discusses various aspects related to dispersion modelling of
865 nanoparticles at five spatial scales: vehicle wake, street canyon, neighbourhood, city
866 and road tunnel. Key flow and mixing characteristics at these scales are discussed.
867 Currently available particle dispersion models, their capabilities and limitations are
868 briefly examined. The relevance of transformation processes such as dilution,
869 emission, nucleation, coagulation, condensation, evaporation, dry and wet depositions
870 at the selected five scales are critically assessed and suggestions for their adequate
871 treatment in dispersion models are outlined. Furthermore, the impact of structural and
872 parametric uncertainties on modelled particle number concentrations is critically
873 discussed.

874 Each spatial scale has distinct flow and mixing characteristics which are complex and
875 thus difficult to generalise (Section 2). Several aerosol dispersion models are currently
876 available for covering the discussed spatial scales (Section 3) but most of them are
877 mainly used for research purposes and are not available commercially for regulatory
878 use. Moreover, the models treating the particle dynamics in detail are complex,
879 resource intensive and require a great amount of additional input information (e.g.
880 type and concentration of condensable species or size dependent chemical
881 composition of nanoparticles), which is not readily available for routine use. It is
882 therefore necessary to identify the relevant key transformation processes at different
883 spatial scales for reducing complexity in model structure and the amount of input
884 information required. The discussion presented in Section 4 indicated that,
885 irrespective of any spatial scale, emission and dilution are crucial processes that need
886 to be modelled in detail before considering the aerosol dynamics. Dilution is also the
887 fastest process at any spatial scale, except for road tunnel environment where dilution

888 is impeded by limited air flow (Ketzel and Berkowicz, 2004). However, sink
889 processes such as coagulation and dry deposition play an important role in road tunnel
890 modelling (Sturm et al., 2003). Generally, other transformation processes become
891 progressively slower with time after emissions are released. For instance, at urban
892 rooftop and city scale the dilution is sufficiently slow to allow coagulation, deposition
893 and condensation to alter the size distribution; these processes need to be considered
894 in urban scale dispersion models (Table 3). Under some conditions (e.g. rapid
895 dilution, initial particles larger than 10 nm), particle dynamics may be disregarded for
896 street scale modelling because the competing influences of these processes have
897 negligible net effects on ToN concentrations (Section 4.6).

898 Aerosol dispersion models are affected by similar uncertainties (structural and
899 parametric) to those of gaseous dispersion models (Vardoulakis et al., 2002) in
900 addition to the uncertainties caused by inappropriate treatment of particle
901 transformation processes. One of the major parametric uncertainties in ToN emission
902 modelling originates in the estimation of PNEFs (Section 5.2). More coherence in
903 their estimation methods is required for obtaining consistent emission factors and
904 reducing the differences between modelled and measured ToN concentrations.

905 Research questions that need further attention related to the dispersion modelling of
906 particle number concentrations include: (i) what prediction accuracy should be
907 acceptable for modelling purposes at various spatial scale (e.g. $\pm 10\%$ of measured
908 data, within a factor of 2 or more), and (ii) which of the uncertainties play a dominant
909 role in the model prediction (e.g. the representation of certain transformation
910 processes, or the inputs provided). Since limited information is available on scientific
911 evaluation, verifications and validations of particle dispersion models, any of the
912 above questions can not be answered precisely. The review qualitatively assesses the
913 relative importance of various transformation processes. Further work can include
914 harmonisation of various model outputs through their inter-comparison under a range
915 of data sets for quantitatively evaluating and establishing the relative importance of
916 particle transformation processes at different urban scales. However, the major
917 practical constraint remains the easy accessibility of currently available particle
918 dispersion models which are mainly used for research purposes by individual groups.

919 The greater number of long-term nanoparticle measurements (including number and
920 size distributions) and the easy accessibility of that data to the scientific community
921 would help to evaluate the performance of particle dispersion models, and to reduce
922 structural and parametric uncertainties. Moreover, there is a need for establishing a
923 standard measurement methodology for the PNEFs that can be readily used for the
924 dispersion modelling of nanoparticles. Developing the capabilities of existing particle
925 dispersion models through comprehensive performance evaluation, and reducing
926 uncertainties by appropriately treating particle dynamics at different urban scales and
927 providing accurate input information are essential steps for accurately predicting ToN
928 concentrations and developing mitigation policies for urban areas.

929 **7. Acknowledgements**

930 PK thanks the EPSRC for the award of a research grant EP/H026290/1 which
931 focuses on the measurements and dispersion modelling of nanoparticles in the wake
932 of moving vehicles. Rex Britter was funded in part by the Singapore National
933 Research Foundation (NRF) through the Singapore-MIT Alliance for Research and

934 Technology (SMART) Center for Environmental Sensing and Modeling (CENSAM)
935 and Future Urban Mobility (FM) programmes.

936 **8. References**

- 937 Abu-Allaban, M., Coulomb, W., Gertler, A.W., Gillies, J., Poerson, W.R., Rogers,
938 C.F., Sagebiel, J.C., and Tarnay, L. (2002). Exhaust particle size distribution
939 measurements at the Tuscarora Mountain Tunnel. *Aerosol Science and*
940 *Technology*, 36, 771-789.
- 941 Albriet, B., Sartelet, K.N., Lacour, S., Carissimo, B., and Seigneur, C. (2010).
942 Modelling aerosol number distributions from a vehicle exhaust with an aerosol
943 CFD model. *Atmospheric Environment*, 44, 1126-1137.
- 944 Andersen, Z.J., Ketzler, M., Loft, S., and Raaschou-Nielsen, O. (2010). Association
945 between short-term exposure to ultrafine particles and hospital admissions for
946 stroke in Copenhagen, Denmark. *European Heart Journal*, 16, 2034-2040.
- 947 Andersen, Z.J., P., W., Raaschou-Nielsen, O., Ketzler, M., Scheike, T., and Loft, S.
948 (2008). Size Distribution and Total Number Concentration of Ultrafine and
949 Accumulation Mode Particles and Hospital Admissions in Children and Elderly in
950 Copenhagen. *Occupational and Environmental Medicine*, 65, 458-466.
- 951 Andronache, C. (2005). Precipitation removal of ultrafine aerosol particles from the
952 atmospheric boundary layer. *Journal of Geophysical Research*, 09, D16S07,
953 doi:10.1029/2003JD004050.
- 954 Arnold, F., Pirjola, L., Aufmhoff, H., Schuck, T., Lähde, T., and Hämeri, K. (2006).
955 First gaseous sulphuric acid detection in automobile exhaust: Implications for
956 volatile nano-particle formation and health risk. *Atmospheric Environment*, 40,
957 7097-7105.
- 958 Baker, C.J. (2001). Flow and dispersion in ground vehicle wakes. *Journal of Fluids*
959 *and Structures*, 15, 1031-1060.
- 960 Bari, S., and Naser, J. (2010). Simulation of airflow and pollution levels caused by
961 severe traffic jam in a road tunnel. *Tunnelling and Underground Space*
962 *Technology*, 25, 70-77.
- 963 Barlow, J.F., Harman, I.N., and Belcher, S.E. (2004). Scalar fluxes from urban street
964 canyons. Part I: Laboratory simulation. *Boundary-Layer Meteorology*, 113, 369-
965 385.
- 966 Beddows, D.C.S., and Harrison, R.M. (2008). Comparison of average particle number
967 emission factors for heavy and light duty vehicles derived from rolling chassis
968 dynamometer and field studies. *Atmospheric Environment*, 42, 7954-7966.
- 969 Belcher, S.E. (2005). Mixing and transport in urban areas. *Philosophical Transactions*
970 *of The Royal Society A*, 363, 2947-2968.
- 971 Bellasio, R. (1997). Modelling traffic air pollution in road tunnels. *Atmospheric*
972 *Environment*, 31, 1539-1551.
- 973 Berkowicz, R. (2000). Operational street pollution model-a parameterized street
974 pollution model. *Environmental Monitoring and Assessment*, 65, 323-331.
- 975 Bottema, M. (1997). Urban roughness modeling in relation to pollutant dispersal.
976 *Atmospheric Environment*, 31, 3059-3075.
- 977 Britter, R.E., Di Sabatino, S., Caton, F., Cooke, K.M., Simmonds, P.G., and Nickless,
978 G. (2002). Results from Three Field Tracer Experiments on the Neighbourhood
979 Scale in the City of Birmingham UK. *Water, Air, & Soil Pollution: Focus*, 2, 79-
980 90.
- 981 Britter, R.E., and Hanna, S.R. (2003). Flow and dispersion in urban areas. *Annual*
982 *Review of Fluid Mechanics*, 35, 469-496.

983 Brugge, D., Durant, J.L., and Rioux, C. (2007). Near-highway pollutants in motor
984 vehicle exhaust: A review of epidemiologic evidence of cardiac and pulmonary
985 health risks. *Environmental Health*, 6, 23.

986 Carpentieri, M., Kumar, P., and Robins, A. (2010). An overview of experimental
987 results and dispersion modelling of nanoparticles in the wake of moving
988 vehicles. *Environmental Pollution*, 159, 685-693.

989 Carpentieri, M., and Kumar, P. (2011). Ground-fixed and on-board measurements of
990 nanoparticles in the wake of a moving vehicle. *Atmospheric Environment*, revised
991 manuscript under review.

992 Caton, F., Britter, R.E., and Dalziel, S. (2003). Dispersion mechanisms in a street
993 canyon. *Atmospheric Environment*, 37, 693-702.

994 Chan, T.L., Liu, Y.H., and Chan, C.K. (2010). Direct quadrature method of moments
995 for the exhaust particle formation and evolution in the wake of the studied ground
996 vehicle. *Journal of Aerosol Science*, 41, 553-568.

997 Charron, A., and Harrison, R.M. (2003). Primary particle formation from vehicle
998 emissions during exhaust dilution in the road side atmosphere. *Atmospheric
999 Environment*, 37, 4109-4119.

1000 Cheng, Y.-H., Liu, Z.-S., and Chen, C.-C. (2010). On-road measurements of ultrafine
1001 particle concentration profiles and their size distributions inside the longest
1002 highway tunnel in Southeast Asia. *Atmospheric Environment*, 44, 763-772.

1003 Coceal, O., and Belcher, S. (2005). Mean winds through an inhomogeneous urban
1004 canopy. *Boundary-Layer Meteorology*, 115, 47-68.

1005 Corsmeier, U., Imhof, D., Kohler, M., Kühlwein, J., Kurtenbach, R., Petrea, M.,
1006 Rosenbohm, E., Vogel, B., and Vogt, U. (2005). Comparison of measured and
1007 model-calculated real-world traffic emissions. *Atmospheric Environment*, 39,
1008 5760-5775.

1009 COST732. (2005-2009). COST Action 732: Quality assurance and improvement of
1010 micro-scale meteorological models. [http://www.mi.uni-
1011 hamburg.de/Home.484.0.html](http://www.mi.uni-hamburg.de/Home.484.0.html).

1012 COST732. (2010). COST Action 732: Quality assurance and improvement of
1013 microscale meteorological models. Model evaluation case studies: approach and
1014 results, ISBN: 3-00-018312-4, pp. 122.

1015 Dahl, A., Gharibi, A., Swietlicki, E., Gudmundsson, A., Bohgard, M., Ljungman, A.,
1016 Blomqvist, G., and Gustafsson, M. (2006). Traffic-generated emissions of
1017 ultrafine particles from pavement-tire interface. *Atmospheric Environment*, 40,
1018 1314-1323.

1019 De Paul, F.T., and Sheih, C.M. (1986). A tracer study of dispersion in an urban street
1020 canyon. *Atmospheric Environment* 20, 455-459.

1021 Di Sabatino, S. (2005). Flow and pollutant dispersion in urban areas. PhD Thesis,
1022 Cambridge University, Cambridge, UK, pp. 242.

1023 Di Sabatino, S., Kastner-Klein, P., Berkowicz, R., Britter, R.E., and Fedorovich, E. (
1024 2003). The modelling of turbulence from traffic in urban dispersion models - part
1025 I: theoretical considerations. *Environmental Fluid Mechanics* 3, 129-143.

1026 El-Fadel, M., and Hashisho, Z. (2001). Vehicular emissions in roadway tunnels: a
1027 critical review. *Critical Reviews in Environmental Science and Technology*, 31,
1028 125-174.

1029 Eskridge, R.E., and Hunt, J.C.R. (1979). Highway modelling Part I: prediction of
1030 velocity and turbulence fields in the wake of vehicles. *Journal of Applied
1031 Meteorology*, 18, 387-400.

1032 Fushimi, A., Hasegawa, S., Takahashi, K., Fujitani, Y., Tanabe, K., and Kobayashi, S.
1033 (2008). Atmospheric fate of nuclei-mode particles estimated from the number
1034 concentrations and chemical composition of particles measured at roadside and
1035 background sites. *Atmospheric Environment*, 42, 949-959.

1036 Gayev, Y.A., Savory, E. (1999). Influence of street obstructions on flow processes
1037 within urban canyons. *Journal of Wind Engineering and Industrial Aerodynamics*,
1038 82, 89-103.

1039 Geller, M.D., Sardar, S.B., Phuleria, H., Fine, P.M., and Sioutas, C. (2005).
1040 Measurement of particle number and mass concentrations and size distributions in
1041 a tunnel environment. *Environmental Science and Technology*, 39, 8653-8663.

1042 Gertler, A.W., Gillies, J.A., Pierson, W.R., Rogers, C.F., Sagebiel, J.C., Abu-Allaban,
1043 M., Coulombe, W., Tarnay, L., and Cahill, T.A. (2002). Real-world particulate
1044 matter and gaseous emissions from motor vehicles in a highway tunnel. *Health*
1045 *Effects Institute Research Report 107*, 79-92.

1046 Gidhagen, L., Johansson, C., Langner, J., and Foltescu, V.L. (2005). Urban scale
1047 modeling of particle number concentration in Stockholm. *Atmospheric*
1048 *Environment*, 39, 1711-1725.

1049 Gidhagen, L., Johansson, C., Langner, J., and Olivares, G. (2004a). Simulation of
1050 NO_x and ultrafine particles in a street canyon in Stockholm, Sweden. *Atmospheric*
1051 *Environment*, 38, 2029-2044.

1052 Gidhagen, L., Johansson, C., Omstedt, G., Langner, J., and Olivares, G. (2004b).
1053 Model Simulations of NO_x and Ultrafine Particles Close to a Swedish Highway.
1054 *Environmental Science and Technology*, 38, 6730-6740.

1055 Gidhagen, L., Johansson, C., Ström, J., Kristensson, A., Swietlicki, E., Pirjola, L., and
1056 Hansson, H.C. (2003). Model simulation of ultrafine particles inside a road tunnel.
1057 *Atmospheric Environment*, 37, 2023-2036.

1058 Gokhale, S., and Khare, M. (2004). A review of deterministic, stochastic and hybrid
1059 vehicular exhaust emission models. *International Journal of Transport*
1060 *Management*, 2, 59-74.

1061 Gramotnev, G., Brown, R., Ristovski, Z., Hitchins, J., and Morawska, L. (2003a).
1062 Determination of average emission factors for vehicles on a busy road.
1063 *Atmospheric Environment* 37, 465-474.

1064 Gramotnev, G., Brown, R., Ristovski, Z., Hitchins, J., and Morawska, L. (2003b).
1065 Determination of average emission factors for vehicles on a busy road.
1066 *Atmospheric Environment*, 37, 465-474.

1067 Gramotnev, G., Ristovski, Z.D., Brown, R.J., and Madl, P. (2004). New methods of
1068 determination of average particle emission factors for two groups of vehicles on a
1069 busy road. *Atmospheric Environment*, 38, 2607-2610.

1070 Grimmond, C.S.B., and Oke, T.R. (1999). Aerodynamic properties of urban areas
1071 derived from analysis of surface form. *Journal of Applied Meteorology*, 38, 1261-
1072 1292.

1073 Hak, C.S., Hallquist, M., Ljungstrom, E., Svane, M., and Pettersson, J.B.C. (2009). A
1074 new approach to in-situ determination of roadside particle emission factors of
1075 individual vehicles under conventional driving conditions. *Atmospheric*
1076 *Environment*, 43, 2481-2488.

1077 Hansen, D., Blahout, B., Benner, D., and Popp, W. (2008). Environmental sampling
1078 of particulate matter and fungal spores during demolition of a building on a
1079 hospital area. *Journal of Hospital Infection*, 70, 259-264.

1080 Heist, D. K., Perry, S.G., and Brixy, L.A. (2009). A wind tunnel study of the effect of
1081 roadway configurations on the dispersion of traffic-related pollution. *Atmospheric*
1082 *Environment*, 43, 5101-5111.

1083 Hinds, W.C. (1999). *Aerosol technology: Properties, behaviour and measurement of*
1084 *airborne particles*. John Wiley & Sons, UK, pp. 483.

1085 Holmes, K.J., Graham, J.A., McKone, T., and Whipple, C. (2009). Regulatory Models
1086 and the Environment: Practice, Pitfalls, and Prospects. *Risk Analysis*, 29, 159-
1087 170.

1088 Holmes, N. (2007). A review of particle formation events and growth in the
1089 atmosphere in the various environments and discussion of mechanistic
1090 implications. *Atmospheric Environment* 41, 2183-2201.

1091 Holmes, N.S., and Morawska, L. (2006). A review of dispersion modelling and its
1092 application to the dispersion of particles: An overview of different dispersion
1093 models available. *Atmospheric Environment*, 40, 5902-5928.

1094 Horvath, H. (1994). Atmospheric aerosols, atmospheric optics visibility. *Journal of*
1095 *Aerosol Science* 25, S23-S24.

1096 Hoydysh, W.G., and Dabberdt, W.F. (1998). Kinematics and dispersion
1097 characteristics of flows in asymmetric street canyons. *Atmospheric Environment*,
1098 22, 2677-2689.

1099 Hu, S., Fruin, S., Kozawa, K., Mara, S., Winer, A.M., and Paulson, S.E. (2009).
1100 Aircraft Emission Impacts in a Neighborhood Adjacent to a General Aviation
1101 Airport in Southern California. *Environmental Science and Technology*, 43, 8039-
1102 8045.

1103 Hucho, W.-H. (1987). Aerodynamics of road vehicles. SAE Technical paper, ISBN,
1104 0-7680-0029-7.

1105 Hueglin, C., Buchmann, B., and Weber, R.O. (2006). Long-term observation of real-
1106 world road traffic emission factors on a motorway in Switzerland. *Atmospheric*
1107 *Environment*, 40, 3696-3709.

1108 Hunt, J.C.R., Johnson, G.T., and Watson, I.D. (1992). An investigation of three
1109 dimensional characteristics of flow regimes within the urban canyon. *Atmospheric*
1110 *Environment*, 26B, 425-432.

1111 Imhof, D., Weingartner, E., Ordoñez, C., Gehrig, R., Hill, M., Buchmann, B., and
1112 Baltensperger, U. (2005a). Real-world emission factors of fine and ultrafine
1113 aerosol particles for different traffic situations in Switzerland. *Environmental*
1114 *Science and Technology*, 39, 8341-8350.

1115 Imhof, D., Weingartner, E., Prevot, A.S.H., Ordonez, C., Kurtenbach, R., Wiesen, P.,
1116 Rodler, J., Sturm, P., McCrae, I., Sjodin, A., and Baltensperger, U. (2005b).
1117 Aerosol and NO_x emission factors and submicron particle number size
1118 distributions in two road tunnels with different traffic regimes. *Atmospheric*
1119 *Chemistry and Physics Discussions*, 5, 5127-5166.

1120 Imhof, D., Weingartner, E., Vogt, U., Dreiseidler, A., Rosenbohm, E., Scheer, V.,
1121 Vogt, R., Nielsen, O.J., Kurtenbach, R., Corsmeier, U., Kohler, M., and
1122 Baltensperger, U. (2005c). Vertical distribution of aerosol particles and NO_x close
1123 to a motorway. *Atmospheric Environment*, 39, 5710-5721.

1124 Jacobson, M.Z. (1997). Development and application of a new air pollution modeling
1125 system--II. Aerosol module structure and design. *Atmospheric Environment*, 31,
1126 131-144.

1127 Jacobson, M.Z. (2001). GATOR-GCMM: A global through urban scale air pollution
1128 and weather forecast model. 1. Model design and treatment of subgrid soil,

1129 vegetation, roads, rooftops, water, sea ice, and snow. *Journal of Geophysical*
1130 *Research*, 106, 5385-5402.

1131 Jacobson, M. Z. (2002). Analysis of aerosol interactions with numerical techniques
1132 for solving coagulation, nucleation, condensation, dissolution, and reversible
1133 chemistry among multiple size distributions. *Journal of Geophysical Research*,
1134 107 (D19), 4366, doi:10.1029/2001JD002044.

1135 Jacobson, M. Z. (2003). Development of mixed-phase clouds from multiple aerosol
1136 size distributions and the effect of the clouds on aerosol removal. *Journal of*
1137 *Geophysical Research*, 108 (D8), 4245, doi:10.1029/2002JD002691.

1138 Jacobson, M.Z., and Seinfeld, J.H. (2004). Evolution of nanoparticle size and mixing
1139 state near the point of emission. *Atmospheric Environment*, 38, 1839-1850.

1140 Jacobson, M.Z. (2005). *Fundamentals of atmospheric modeling*. Cambridge
1141 University Press, 2nd Edition, pp. 784.

1142 Jacobson, M.Z., Kittelson, D.B., and Watts, W.F. (2005). Enhanced coagulation due
1143 to evaporation and its effect on nanoparticle evolution. *Environmental Science and*
1144 *Technology*, 39 9486-9492.

1145 Jamriska, M., and Morawska, L. (2001). A model for determination of motor vehicle
1146 emission factors from on-road measurements with a focus on sub micrometer
1147 particles. *Science of the Total Environment* 264, 241–255.

1148 Jamriska, M., Morawska, L., Thomas, S., and Congrong, H. (2004). Diesel bus
1149 emissions measured in a tunnel study. *Environmental Science and Technology*,
1150 38, 6701-6709.

1151 Jayaratne, E.R., Ristovski, Z.D., Meyer, N., and Morawska, L. (2009). Particle and
1152 gaseous emissions from compressed natural gas and ultralow sulphur diesel-
1153 fuelled buses at four steady engine loads. *Science of The Total Environment*, 407,
1154 2845-2852.

1155 Jones, A.M., and Harrison, R.M. (2006). Estimation of the emission factors of particle
1156 number and mass fractions from traffic at a site where mean vehicle speeds vary
1157 over short distances. *Atmospheric Environment*, 40, 7125-7137.

1158 Kastner-Klein, P., Fedorovich, E., Ketznel, M., Berkowicz, R., and Britter, R. (2003).
1159 The modelling of turbulence from traffic in urban dispersion models - Part II:
1160 evaluation against laboratory and full-scale concentration measurements in street
1161 canyons. *Environmental Fluid Mechanics* 3, 145-172.

1162 Keogh, D.U., Ferreira, L., and Morawska, L. (2009). Development of a particle
1163 number and particle mass vehicle emissions inventory for an urban fleet.
1164 *Environmental Modelling & Software*, 24, 1323-1331.

1165 Kerminen, V.-M., Lehtinen, K.J., Anttila, T., and Kulmala, M. (2004). Dynamics of
1166 atmospheric nucleation mode particles: a timescale analysis. *Tellus*, 56B, 135-146.

1167 Kerminen, V.-M., Pakkanen, T.A., Mäkelä, T., Hillamo, R.E., Rönkkö, T., Virtanen,
1168 A., Keskinen, J., Pirjola, L., Hussein, T., and Hämeri, K. (2007). Development of
1169 particle number size distribution near a major road in Helsinki during an episodic
1170 inversion situation. *Atmospheric Environment*, 41, 1759-1767.

1171 Ketznel, M., and Berkowicz, R. (2004). Modelling the fate of ultrafine particles from
1172 exhaust pipe to rural background: an analysis of time scales for dilution,
1173 coagulation and deposition. *Atmospheric Environment*, 38, 2639-2652.

1174 Ketznel, M., and Berkowicz, R. (2005). Multi-plume aerosol dynamics and transport
1175 model for urban scale particle pollution. *Atmospheric Environment*, 39, 3407-
1176 3420.

1177 Ketznel, M., Hansson, H.C., Berkowicz, R., Palmgren, F., Glasius, M., Løfstrøm, P.,
1178 and et al. (2007). Final report on the NMR Project: NORPAC - Validated models

1179 describing Nordic urban and regional concentration of particles and organic /
1180 elemental carbon (OC/EC). Nordic council of Ministers Working Group Marine &
1181 Air, pp. 44. Download from:
1182 http://www2.dmu.dk/AtmosphericEnvironment/norpac/Downloads/NORPAC_FinalReport_Dec2007.pdf.
1183

1184 Ketznel, M., Wahlin, P., Berkowicz, R., and Palmgren, F. (2003). Particle and trace gas
1185 emission factors under urban driving conditions in Copenhagen based on street
1186 and roof-level observations. *Atmospheric Environment* 37, 2735-2749.

1187 Kim, J.J., and Baik, J.J. (2001). Urban street canyon flows with bottom heating.
1188 *Atmospheric Environment* 35, 3395-3404.

1189 Kirchstetter, T.W., Harley, R.A., Kriesberg, N.M., Stolzenburg, M.R., and Hering,
1190 S.V. (2002). Corrigendum to "On-road measurement of fine particle and nitrogen
1191 oxide emissions from light- and heavy-duty motor vehicles". *Atmospheric*
1192 *Environment* 36, 6059.

1193 Kittelson, D.B. (1998). Engines and nano-particles: a review. *Journal of Aerosol*
1194 *Science*, 29, 575-588.

1195 Kittelson, D.B., Kadue, P.A., Scherrer, H.C., and Lovrien, R. (1988). Characterization
1196 of diesel particles in the atmosphere. Final Report, Coordinating Research
1197 Council.

1198 Kittelson, D.B., Watts, W.F., and Johnson, J.P. (2004). Nanoparticle emissions on
1199 Minnesota highways. *Atmospheric Environment* 38, 9-19.

1200 Korhonen, H., Lehtinen, K.E.J., and Kulmala, M. (2004). Multicomponent aerosol
1201 dynamics model UHMA: model development and validation. *Atmospheric*
1202 *Chemistry and Physics*, 4, 757-771.

1203 Kovar-Pankus, A., Moulinneuf, L., Savory, E., Abdelqari, A., Sini, J.-F., Rosant, J.-
1204 M., Robins, A., and Toy, N.A. (2002). Wind tunnel investigation of the influences
1205 of solar-induced wall-heating on the flow regime within a simulated urban street
1206 canyon. *Water, Air and Soil Pollution*, 2, 555-571.

1207 Kristensson, A., Johansson, C., Westerholm, R., Swietlicki, E., Gidhagen, L.,
1208 Wideqvist, U., and Vesely, V. (2004). Real-world traffic emission factors of gases
1209 and particles measured in a road tunnel in Stockholm, Sweden. *Atmospheric*
1210 *Environment* 38, 657-673.

1211 Kuhn, T., Krudysz, M., Zhu, Y., Fine, P.M., Hinds, W.C., Froines, J., and Sioutas, C.
1212 (2005). Volatility of indoor and outdoor ultrafine particulate matter near a
1213 freeway. *Journal of Aerosol Science*, 36, 291-302.

1214 Kulmala, M., Vehkamäki, H., Petaja, T., Dal Maso, M., Lauri, A., Kerminen, V.-M.,
1215 Birmili, W., and McMurry, P.H. (2004). Formation and growth rates of ultrafine
1216 particles: a review of observations. *Journal of Aerosol Science*, 35, 143-176.

1217 Kulmala, M., Riipinen, I., Sipilä, M., Manninen, H. E., Petäjä, T., Junninen, H., Dal
1218 Maso, M., Mordas, G., Mirme, A., Vana, M., Hirsikko, A., Laakso, L., Harrison,
1219 R.M., Hanson, I., Leung, C., Lehtinen, K.E.J., and Kerminen, V.-M. (2007).
1220 Toward direct measurement of atmospheric nucleation, *Science*, 318, 89-92.

1221 Kumar, P., Fennell, P., and Britter, R. (2008a). Effect of wind direction and speed on
1222 the dispersion of nucleation and accumulation mode particles in an urban street
1223 canyon. *Science of the Total Environment*, 402, 82-94.

1224 Kumar, P., Fennell, P., and Britter, R. (2008b). Measurements of particles in the 5-
1225 1000 nm range close to road level in an urban street canyon. *Science of the Total*
1226 *Environment*, 390, 437-447.

- 1227 Kumar, P., Fennell, P., Langley, D., and Britter, R. (2008c). Pseudo-simultaneous
 1228 measurements for the vertical variation of coarse, fine and ultra fine particles in an
 1229 urban street canyon. *Atmospheric Environment*, 42, 4304-4319.
- 1230 Kumar, P., Fennell, P., Hayhurst, A., and Britter, R.E. (2009a). Street versus rooftop
 1231 level concentrations of fine particles in a Cambridge street canyon. *Boundary-
 1232 Layer Meteorology*, 131, 3-18.
- 1233 Kumar, P., Garmory, A., Ketzel, M., Berkowicz, R., and Britter, R. (2009b).
 1234 Comparative study of measured and modelled number concentrations of
 1235 nanoparticles in an urban street canyon. *Atmospheric Environment*, 43, 949-958.
- 1236 Kumar, P., Robins, A., and Britter, R. (2009c). Fast response measurements for the
 1237 dispersion of nanoparticles in a vehicle wake and in a street canyon. *Atmospheric
 1238 Environment*, 43, 6110-6118.
- 1239 Kumar, P., Fennell, P., and Robins, A. (2010a). Comparison of the behaviour of
 1240 manufactured and other airborne nanoparticles and the consequences for
 1241 prioritising research and regulation activities. *Journal of Nanoparticle Research*,
 1242 12, 1523-1530.
- 1243 Kumar, P., Robins, A., and ApSimon, H. (2010b). Nanoparticle emissions from
 1244 biofuelled vehicles - their characteristics and impact on the number-based regulation
 1245 of atmospheric particles. *Atmospheric Science Letters*, 11, 327-331.
- 1246 Kumar, P., Robins, A., Vardoulakis, S., and Britter, R. (2010c). A review of the
 1247 characteristics of nanoparticles in the urban atmosphere and the prospects for
 1248 developing regulatory control. *Atmospheric Environment*, 44, 5035-5052.
- 1249 Kumar, P., Gurjar, B.R., Nagpure, A., and Harrison, R.M. (2011a). Preliminary
 1250 estimates of nanoparticle number emissions from road vehicles in megacity
 1251 Delhi and associated health impacts. *Environmental Science and Technology*, in
 1252 press, doi:10.1021/es2003183.
- 1253 Kumar, P., Robins, A., Vardoulakis, S., and Quincey, P. (2011b). Technical
 1254 challenges in tackling regulatory concerns for urban atmospheric nanoparticles.
 1255 *Particuology*, revised manuscript under review.
- 1256 Laakso, L., Grönholm, T., Rannik, Ü., Kosmale, M., Fiedler, V., Vehkamäki, H., and
 1257 Kulmala, M. (2003). Ultrafine particle scavenging coefficients calculated from 6
 1258 years field measurements. *Atmospheric Environment*, 37, 3605-3613.
- 1259 Lee, K.W., and Gieseke, J.A. (1994). Deposition of particles in turbulent flow pipes.
 1260 *Journal of Aerosol Science*, 25, 699-704.
- 1261 Li, X.-X., Liu, C.-H., Leung, D.Y.C., and Lam, K.M. (2006). Recent progress in CFD
 1262 modelling of wind field and pollutant transport in street canyons. *Atmospheric
 1263 Environment*, 40, 5640-5658.
- 1264 Li, Y., Suriyawong, A., Daukoru, M., Zhuang, Y., and Biswas, P. (2009).
 1265 Measurement and capture of fine and ultrafine particles from a pilot-scale
 1266 pulverized coal combustor with an electrostatic precipitator. *Journal of Air and
 1267 Waste Management Association*, 59, 553-559.
- 1268 Lohmeyer, A., Mueller, W.J., and Baechlin, W. (2002). A comparison of street
 1269 canyon concentration predictions by different modellers: final results now
 1270 available from the Podbi-exercise. *Atmospheric Environment*, 36, 157-158.
- 1271 Louka, P., Belcher, S.E., and Harrison, R.G. (2000). Coupling between air flow in
 1272 streets and the well-developed boundary layer aloft. *Atmospheric Environment*,
 1273 34, 2613-2621.
- 1274 Louka, P., Vachon, G., Sini, J.F., Mestayer, P.G., and Rosant, J.M. (2002). Thermal
 1275 effects on the airflow in a street canyon-Nantes '99 experimental results and
 1276 model simulation. *Water, Air and Soil Pollution*, 2, 351-364.

1277 MDS. (2010). Model Documentation System (MDS) of European Topic Centre on Air
1278 and Climate change Download from:
1279 <http://pandora.meng.auth.gr/mds/strquery.php?wholedb>.

1280 Milionis, A.E., and Davies, T.D. (1994). Regression and stochastic models for air
1281 pollution--I. Review, comments and suggestions. *Atmospheric Environment*, 28,
1282 2801-2810.

1283 Møller, P., Folkmann, J.K., Forchhammer, L., Bräuner, E.V., Danielsen, P.H., Risom,
1284 L., and Loft, S. (2008). Air pollution, oxidative damage to DNA, and
1285 carcinogenesis. *Cancer Letters*, 266, 84-97.

1286 Morawska, L., Bofinger, N.D., Kocis, L., and Nwankwoala, A. (1998).
1287 Submicrometer and supermicrometer particles from diesel vehicle emissions.
1288 *Environmental Science and Technology*, 32, 2033–2042.

1289 Morawska, L., Jamriska, M., Thomas, S., Ferreira, L., Mengersen, K., Wraith, D., and
1290 McGregor, F. (2005). Quantification of particle number emission factors for motor
1291 vehicles from on road measurements. *Environmental Science and Technology* 39,
1292 9130-9139.

1293 Murr, L.E., and Garza, K.M. (2009). Natural and anthropogenic environmental
1294 nanoparticulates: Their microstructural characterization and respiratory health
1295 implications. *Atmospheric Environment*, 43, 2683-2692.

1296 Nel, A., Xia, T., Madler, L., and Li, N. (2006). Toxic Potential of Materials at the
1297 Nanolevel. *Science*, 311, 622-627.

1298 Olivares, G., Johansson, C., Strom, J., and Hansson, H.-C. (2007). The role of
1299 ambient temperature for particle number concentrations in a street canyon.
1300 *Atmospheric Environment*, 41, 2145-2155.

1301 Petroff, A., and Zhang, L. (2010). Development and validation of a size-resolved
1302 particle dry deposition scheme for applications in aerosol transport models.
1303 *Atmospheric Chemistry and Physics Discussions*, 3, 1317-1357.

1304 Pey, J., Querol, X., Alastuey, A., Rodríguez, S., Putaud, J.P., and Van Dingenen, R.
1305 (2009). Source apportionment of urban fine and ultra fine particle number
1306 concentration in a Western Mediterranean city. *Atmospheric Environment*, 43,
1307 4407-4415.

1308 Pirjola, L. (1999). Effects of the increased uv radiation and biogenic voc emissions on
1309 ultrafine sulphate aerosol formation. *Journal of Aerosol Science*, 30, 355-367.

1310 Pirjola, L., and Kulmala, M. (2000). Aerosol dynamical model MULTIMONO.
1311 *Boreal Environment Research*, 5, 361-374.

1312 Pirjola, L., and Kulmala, M. (2001). Development of particle size and composition
1313 distributions with a novel aerosol dynamics model. *Tellus Series B-Chemical and*
1314 *Physical Meteorology*, 53, 491-509.

1315 Pohjola, M., Pirjola, L., Kukkonen, J., and Kulmala, M. (2003). Modelling of the
1316 influence of aerosol processes for the dispersion of vehicular exhaust plumes in
1317 street environment. *Atmospheric Environment*, 37, 339-351.

1318 Pirjola, L., Tsyro, S., Tarrason, L., and Kulmala, M. (2003). A monodisperse aerosol
1319 dynamics module – a promising candidate for use in the Eulerian long-range
1320 transport model. *Journal of Geophysical Research*, 108 (D9), 4258,
1321 doi:10.1029/2002JD002867.

1322 Pirjola, L., Lehtinen, K.E.J., Hansson, H.-C., and Kulmala, M. (2004). How important
1323 is nucleation in regional/global modelling. *Geophysical Research Letters*, 31,
1324 L12109, doi:10.1029/2004GL019525.

1325 Pohjola, M.A., Pirjola, L., Karppinen, A., Härkönen, J., Korhonen, H., Hussein, T.,
1326 Ketznel, M., and Kukkonen, J. (2007). Evaluation and modelling of the size

1327 fractionated aerosol particle number concentration measurements nearby a major
1328 road in Helsinki - Part I: Modelling results within the LIPIKA project.
1329 Atmospheric Chemistry and Physics, 7 4065-4080.

1330 Pope III, C.A., and Dockery, D.W. (2006). Health effects of fine particulate air
1331 pollution: Lines that connect. Journal of Air & Waste Management Association
1332 56, 707-742.

1333 Prati, M.V., and Costagliola, M.A. (2008). Particle emission factors of different
1334 vehicle classes. 31st Meeting on Combustion, Combustion Institute, pp. 1-8,
1335 <http://www.combustioninstitute.it/proc/proc2008/data/papers/IV/IV-2008.pdf>.

1336 Raupach, M.R., Thom, A.S., and Edwards, I. (1980). A wind-tunnel study of turbulent
1337 flow close to regularly arrayed rough surfaces. Boundary-Layer Meteorology, 18,
1338 373-397.

1339 Rijkeboer, R., Bremmers, D., Samaras, Z., and Ntziachristos, L. (2005). Particulate
1340 matter regulation for two-stroke two wheelers: Necessity or haphazard legislation?
1341 Atmospheric Environment, 39, 2483-2490.

1342 Ristovski, Z.D., Jayaratne, E.R., Lim, M., Ayoko, G.A., and Morawska, L. (2006).
1343 Influence of Diesel Fuel Sulfur on Nanoparticle Emissions from City Buses.
1344 Environmental Science & Technology, 40, 1314-1320.

1345 Ristovski, Z.D., Jayaratne, E.R., Morawska, L., Ayoko, G.A., and Lim, M. (2005).
1346 Particle and carbon dioxide emissions from passenger vehicles operating on
1347 unleaded petrol and LPG fuel. Science of The Total Environment, 345, 93-98.

1348 Ristovski, Z.D., Morawska, L., Ayoko, G.A., Jayaratne, E.R., and Lim, M. (2002).
1349 Final report of a comparative investigation of particle and gaseous emissions from
1350 twelve in-service B.C.C buses operating on 50 and 500ppmsulphur diesel fuel.
1351 Queensland University of Technology, Brisbane, Australia.

1352 Ristovski, Z.D., Morawska, L., Ayoko, G.A., Johnson, G., Gilbert, D., and
1353 Greenaway, C. (2004). Science of the Total Environment. Emissions from a
1354 vehicle fitted to operate on either petrol or compressed natural gas, 323, 179-194.

1355 Robertson, L., Langner, J., and Engardt, M. (1999). An Eulerian limited-area
1356 atmospheric transport model. Journal of Applied Meteorology, 38, 190-210.

1357 Roldin, P., Swietlicki, E., Massling, A., Kristensson, A., Londahl, J.L., Eriksson, A.,
1358 Pagels, J., and Gustafsson, S. (2010a). Aerosol ageing in an urban plume–
1359 implications for climate and health. Atmospheric Chemistry and Physics
1360 Discussions, 10, 18731–18780.

1361 Roldin, P., Swietlicki, E., Schurgers, G., Arneth, A., Lehtinen, K.E.J., Boy, M., and
1362 Kulmala, M. (2010b). Development and evaluation of the aerosol dynamic and
1363 gas phase chemistry model ADCHEM. Atmospheric Chemistry and Physics
1364 Discussions, 10, 18661-18730.

1365 Rotach, M.W. (1993a). Turbulence close to a rough urban surface. Part I: Reynolds
1366 stress. Boundary-Layer Meteorology, 65, 1-28.

1367 Rotach, M.W. (1993b). Turbulence close to a rough urban surface. Part II: variances
1368 and gradients. Boundary-Layer Meteorology, 66, 75-92.

1369 Rönkkö, T., Virtanen, A., Kannosto, J., Keskinen, J., Lappi, M., and Pirjola, L.
1370 (2007). Characteristics of nucleation mode particles in exhaust of Euro IV heavy
1371 duty diesel vehicle. Environmental Science and Technology, 41, 6384-6389.

1372 Sakurai, H., Tobias, K., Park, D., Zarling, K.S., Docherty, D., Kittelson, D.B.,
1373 McMurry, P.H., and Zeimann, P.J. (2003). On-line measurements of diesel
1374 nanoparticle composition and volatility. Atmospheric Environment, 37, 1199-
1375 1210.

1376 Schack Jr, C.J., Pratsinis, S.E., and Friedlander, S.K. (1985). A general correlation for
1377 deposition of suspended particles from turbulent gases to completely rough
1378 surfaces. *Atmospheric Environment* (1967), 19, 953-960.

1379 Seigneur, C. (2009). Current understanding of ultra fine particulate matter emitted
1380 from mobile sources. *Journal of the Air & Waste Management Association*, 59, 3-
1381 17.

1382 Seinfeld, J.H., and Pandis, S., N. (2006). *Atmospheric Chemistry and Physics, from*
1383 *Air Pollution to Climate Change*. John Wiley, New York, pp. 1203.

1384 Sharma, N., Chaudhry, K.K., and Rao, C.C.V. (2004). Vehicular pollution prediction
1385 modelling: a review of highway dispersion models. *Transport Reviews: A*
1386 *Transnational Transdisciplinary Journal*, 24, 409 - 435.

1387 Sharma, P., and Khare, M. (2001). Modelling of vehicular exhausts - a review.
1388 *Transportation Research Part D*, 6, 179-198.

1389 Shi, P.J., Khan, A.A., and Harrison, R.M. (1999). Measurements of ultra fine particle
1390 concentration and size distribution in the urban atmosphere. *Science of the Total*
1391 *Environment* 235, 51-64.

1392 Sini, J.-F., Anquetin, S., and Mestayer, P.G. (1996). Pollutant dispersion and thermal
1393 effects in urban street canyons. *Atmospheric Environment*, 30, 2659-2677.

1394 Smits, A.J., and Wood, D.H. (1985). The response of turbulent boundary layers to
1395 sudden perturbation. *Annual Review of Fluid Mechanics*, 17, 321-358.

1396 Solazzo, E., Vardoulakis, S., and Cai, X. (2007). Evaluation of traffic-producing
1397 turbulence schemes within operating schemes within operational street
1398 pollution models using road side measurements *Atmospheric Environment*,
1399 41, 5357-5370.

1400 Solazzo, E., Cai, X., and Vardoulakis, S. (2008). Modelling wind flow and vehicle-
1401 induced turbulence in urban streets. *Atmospheric Environment*, 42, 4918-4931.

1402 Solazzo, E., Vardoulakis, S., and Cai, X. (2007). Evaluation of traffic-producing
1403 turbulence schemes within operating schemes within operational street pollution
1404 models using road side measurements *Atmospheric Environment*, 41, 5357-5370.

1405 Strawa, A.W., Kirchstetter, T.W., Hallar, A.G., Ban-Weiss, G.A., McLaughlin, J.P.,
1406 Harley, R.A., and Lunden, M.M. (2010). Optical and physical properties of
1407 primary on-road vehicle particle emissions and their implications for climate
1408 change. *Journal of Aerosol Science*, 41, 36-50.

1409 Sturm, P.J., Baltensperger, U., Bacher, M., Lechner, B., Hausberger, S., Heiden, B.,
1410 Imhof, D., Weingartner, E., Prevot, A.S.H., Kurtenbach, R., and Wiesen, P.
1411 (2003). Roadside measurements of particulate matter size distribution.
1412 *Atmospheric Environment*, 37, 5273-5281.

1413 Uhrner, U., von Löwis, S., Vehkamäki, H., Wehner, B., Bräsel, S., Hermann, M.,
1414 Stratmann, F., Kulmala, M., and Wiedensohler, A. (2007). Dilution and aerosol
1415 dynamics within a diesel car exhaust plume-CFD simulations of on-road
1416 measurement conditions. *Atmospheric Environment*, 41, 7440-7461.

1417 Vardoulakis, S., Fisher, B.E.A., Gonzalez-Flesca, N., and Pericleous, K. (2002).
1418 Model sensitivity and uncertainty analysis using roadside air quality
1419 measurements. *Atmospheric Environment*, 36, 2121-2134.

1420 Vardoulakis, S., Fisher, B.R.A., Pericleous, K., and Gonzalez-Flesca, N. (2003).
1421 Modelling air quality in street canyons: a review. *Atmospheric Environment*, 37,
1422 155-182.

1423 Vardoulakis, S., Valiantis, M., Milner, J., and ApSimon, H. (2007). Operational air
1424 pollution modelling in the UK – Street canyon applications and challenges.
1425 *Atmospheric Environment*, 41, 4622-4637.

1426 Vardoulakis, S., R., D., Richards, K., Hamlyn, D., Camilleri, G., Weeks, M., Sini, J.-
1427 F., Britter, R., Borrego, C., Schatzmann, M., and Moussiopoulos, N. (2011).
1428 Numerical model inter-comparison for wind flow and turbulence around single
1429 block buildings. *Environmental Modelling & Assessment*, 16, 169-181.

1430 Vignati, E., Berkowicz, R., Palmgren, F., Lyck, E., and Hummelshoj, P. (1999).
1431 Transformation of size distributions of emitted particles in streets. *Science of the*
1432 *Total Environment* 235, 37-49.

1433 Vogt, R., Scheer, V., Casati, R., and Benter, T. (2003). On-road measurement of
1434 particle emission in the exhaust plume of a diesel passenger car. *Environmental*
1435 *Science and Technology*, 37, 4070-4076.

1436 Wählín, P. (2009). Measured reduction of kerbside ultrafine particle number
1437 concentrations in Copenhagen. *Atmospheric Environment*, 43, 3645-3647.

1438 Wählín, P., Palmgren, F., and Van Dingenen, R. (2001). Experimental studies of
1439 ultrafine particles in streets and the relationship of traffic. *Atmospheric*
1440 *Environment*, 35, S63-S69.

1441 Wang, Y., and Zhang, K.M. (2009). Modeling near-road air quality using a
1442 computational fluid dynamics (CFD) model, CFD-VIT-RIT. *Environmental*
1443 *Science and Technology*, 43, 7778-7783.

1444 Wang, F., Ketzel, M., Ellermann, T., Wählín, P., Jensen, S.S., Fang, D., and Massling,
1445 A. (2010a). Particle number, particle mass and NO_x emission factors at a highway
1446 and an urban street in Copenhagen. *Atmospheric Chemistry and Physics*, 10,
1447 2745–2764.

1448 Wang, F., Roldin, P., Massling, A., Kristensson, A., Swietlicki, E., Fang, D., and
1449 Ketzel, M. (2010b). Aerosol dynamics in the Copenhagen urban plume during
1450 regional transport. *Atmospheric Chemistry and Physics Discussions*, 10, 8553–
1451 8594.

1452 Wehner, B., Birmili, W., Gnauk, T., and Wiedensohler, A. (2002). Particle number
1453 size distributions in a street canyon and their transformation into the urban air
1454 background: measurements and a simple model study. *Atmospheric Environment*
1455 36, 2215-2223.

1456 Wehner, B., Uhrner, U., von Löwis, S., Zallinger, M., and Wiedensohler, A. (2009).
1457 Aerosol number size distributions within the exhaust plume of a diesel and a
1458 gasoline passenger car under on-road conditions and determination of emission
1459 factors. *Atmospheric Environment*, 43, 1235-1245.

1460 Wehner, B., and Wiedensohler, A. (2003). Long term measurements of
1461 submicrometer urban aerosols: statistical analysis for correlations with
1462 meteorological conditions and trace gases. *Atmospheric Chemistry Physics*, 3,
1463 867-879.

1464 Xie, X., Huang, Z., Wang, J., and Xie, Z. (2005). Thermal effects on vehicle emission
1465 dispersion in an urban street canyon *Transportation Research Part D:*
1466 *Transport and Environment*, 10, 197-212.

1467 Zhang, K.M., and Wexler, A.S. (2002). Modeling the number distributions of urban
1468 and regional aerosols: theoretical foundations. *Atmospheric Environment*, 36,
1469 1863-1874.

1470 Zhang, K.M., and Wexler, A.S. (2004). Evolution of particle number distribution near
1471 roadways - Part I: analysis of aerosol dynamics and its implications for engine
1472 emission measurement. *Atmospheric Environment*, 38, 6643-6653.

1473 Zhang, K.M., Wexler, A.S., Niemeier, D.A., Zhu, Y.F., Hinds, W.C., and Sioutas, C.
1474 (2005). Evolution of particle number distribution near roadways. Part III: Traffic

1475 analysis and on-road size resolved particulate emission factors. Atmospheric
1476 Environment 39, 4155-4166.
1477 Zhang, K.M., Wexler, A.S., Zhu, Y.F., Hinds, W.C., and Sioutas, C. (2004).
1478 Evolution of particle number distribution near roadways - Part II: the 'Road-to-
1479 Ambient' process. Atmospheric Environment, 38, 6655-6665.
1480 Zhu, Y., and Hinds, W.C. (2005). Predicting particle number concentrations near a
1481 highway based on vertical concentration profile. Atmospheric Environment, 39,
1482 1557-1566.
1483

1484 **Figure Captions**

1485 Fig. 1. Schematic diagram of the flow through and over an urban area (Grimmond and
1486 Oke, 1999). Also are shown various layers in the ABL and horizontally spatially
1487 averaged mean velocity profile (Bottema, 1997).

1488 Fig. 2. Size dependent deposition speed of particles onto the surfaces calculated using
1489 two different equations within a range of typical urban parameters; figure adapted
1490 from Ketznel and Berkowicz (2004).

1491 Fig. 3. Time scales for dilution, coagulation and deposition at different spatial scales.
1492 For each concentration level the process with the smallest time scale is the most
1493 relevant one. For the dilution of the exhaust plume the time scale is very different for
1494 a road tunnel and the ambient atmosphere (e.g. street); figure adapted from Ketznel and
1495 Berkowicz (2004).

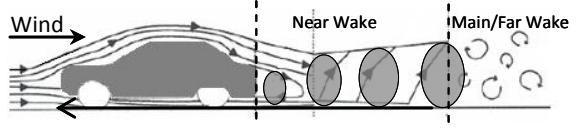
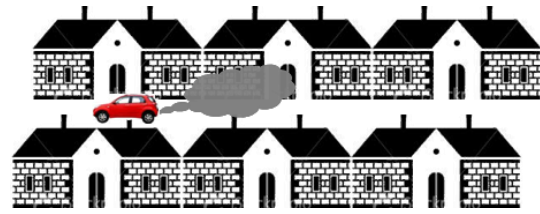
1496 Fig. 4. Measured and corrected (for losses in sampling tubes) particle number
1497 distributions at (a) $z/H = 0.09$, (b) $z/H = 0.19$, (c) $z/H = 0.40$ and (d) $z/H = 0.64$ of an
1498 11.75 m high (H) street canyon; figure adapted from Kumar et al. (2008c). Dotted
1499 lines represent mode fitting curves to corrected particle number distributions. Error
1500 bars show the standard deviation of hourly averaged particle number distributions at
1501 each height; only positive error bars are plotted for the clarity of the figures.

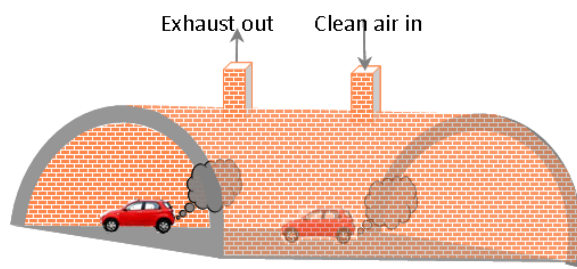
1502 Fig. 5. Inter-comparison of modelled results from the MAT (a, c) and AEROFOR (b,
1503 d) for the test case in Copenhagen; figure adapted from Ketznel et al. (2007). Figs. a
1504 and b show time dependence of the ToN concentration at ground level; results are
1505 from 5 simulations including different aerosol dynamics processes. Figs. c and d show
1506 size distribution calculated with different particle dynamics processes considered.
1507 Note that two different growth rates (GR) considered for the simulation with
1508 condensation; these are 1 and 6 nm h⁻¹ for cases ending with letters Con1 and Con2,
1509 respectively. For comparison the measured size distributions at Lilly Valby (near-
1510 city) and urban rooftop of the H.C. Orsted Institute (HCOE). Simulation time was
1511 12000 s.

1512

1513 **List of Tables**

1514 Table 1. Description of flow and mixing characteristics at various urban scales
 1515 (Belcher, 2005; Britter and Hanna, 2003; Hucho, 1987; Hunt et al., 1992). The
 1516 abbreviations indicate as follows NW (near wake), MW (main/far wake), WPT (wind
 1517 produced turbulence), TPT (traffic produced turbulence), and TCT (thermally
 1518 produced turbulence).

Urban scales	Key flow and mixing features
 <p>Vehicle wake ($L_v \sim 0-20$ m)</p>	<ul style="list-style-type: none"> • Flow is more turbulent in NW region compared with MW region. • TPT is intense in NW and dominate the mixing • Atmospheric turbulence (WPT and TCT) lead the further mixing in MW region
 <p>Street scale ($L_s \sim 100-200$ m)</p>	<ul style="list-style-type: none"> • Flow features and mixing determined by surface roughness below building height • Internal mixing layers below or above the buildings are of order of building or street dimensions • TPT dominate the mixing over the WPT during calm wind conditions • TCT may play role in mixing during hot sunny weather and light winds
 <p>Neighbourhood scale ($L_N \sim 1-2$ km)</p>	<ul style="list-style-type: none"> • Flow and mixing above and between buildings is determined by the turbulence generated by interaction of flows from adjacent canyons, surface and wall roughness, WPT, TPT and TCT. • A growing internal layer of flow can be seen above buildings • Average geometrical features dominate mean flow and mixing
 <p>City scale ($L_C \sim 10-20$ km)</p>	<ul style="list-style-type: none"> • Flow and mixing over buildings is relatively less complex than within the city due to orographic (i.e. surface roughness elements) effects • Mixing below the building heights in the ABL is dominated by surface roughness and the TPT; the atmospheric turbulence (i.e. WPT and TCT) plays a key role in flows over urban canopy



Road tunnels ($L_T \sim 50-5000$ m)

- Flow is generally very turbulent and the mixing is dominated by the TPT and the so-called piston effect generating a mean flow in driving direction of the traffic
- Effect of atmospheric turbulence on the mixing of pollutants is negligible

1519

1520

1521 Table 2. Examples of few urban scale dispersion models that address particle number
 1522 concentrations.

Model	Remarks	Source / Example
OSPM (Operational Street Pollution Model)	<ul style="list-style-type: none"> Predicts particle <i>number</i> concentrations at street scale, but note the OSPM completely neglects particle dynamics 	(Berkowicz, 2000)
UHMA (University of Helsinki Multi Component Aerosol Model)	<ul style="list-style-type: none"> Provides size segregated predictions for number and size distributions between 0.7 nm and 2 μm, with a focus on new particle formation and growth in the atmosphere. 	(Korhonen et al., 2004)
MAT (Multi-plume Aerosol dynamics and Transport)	<ul style="list-style-type: none"> Predicts particle number size distribution in urban environments. It uses a novel multi-plume scheme for vertical dispersion and routines of the sectional aerodynamics models AERO3 (Vignati et al., 1999). 	(Ketzel and Berkowicz, 2005)
MONO32 (Multimono)	<ul style="list-style-type: none"> Simplified version of the Lagrangian type atmospheric chemistry and aerosol dynamics box model MULTIMONO which refers to multi component condensation of different vapours; each size section is assumed to be monodisperse. Can predict the particles between 1 nm and 2.5 μm using optional number of size fractions. Implemented into the EMEP model. 	(Pirjola and Kulmala, 2000; Pirjola et al., 2003; Pohjola et al., 2003)
AEROFOR/AEROFOR2 (Model for Aerosol Formation and dynamics)	<ul style="list-style-type: none"> Lagrangian type sectional box model which includes gas-phase chemical reactions together with aerosol dynamics; predicts number and size distributions of particles, AEROFOR2 also composition size distribution. 	(Pirjola, 1999; Pirjola and Kulmala, 2001)
MATCH (Multi-scale Atmospheric Transport and Chemistry)	<ul style="list-style-type: none"> Eulerian grid-point model which describes the physical and chemical processes that govern emissions, atmospheric transport and dispersion, chemical transformation, wet and dry deposition of pollutants; particle dynamics modules for predicting number and size distributions was included. 	(Gidhagen et al., 2005; Robertson et al., 1999)
GATOR-GCMM (Gas, Aerosol, Transport, Radiation, General circulation and mesoscale meteorological)	<ul style="list-style-type: none"> GATOR-GCMM is derived from GATORG (global) and GATORM (regional) models; this is a single, unified model and can be switched to run global, regional or nested mode with/without gases, aerosols, radiation, meteorology, transport, deposition, cloud physics, surface processes, etc. 	(Jacobson, 1997; Jacobson, 2001) and references therein

	<ul style="list-style-type: none"> • The model is capable of treating nearly all the size and composition resolved aerosol processes (emissions, nucleation, coagulation, condensation, dry deposition and sedimentation). 	
ADCHEM (Aerosol Dynamics, gas and particle phase CHEMistry)	<ul style="list-style-type: none"> • Unlike Lagrangian box-models (0-space dimensions), the ADCEHM treats both vertical and horizontal dispersion perpendicular to an air mass trajectory (2-space dimension). • The model is suitable for local to regional scales to predict number and size distributions in the 1.5 to 2500 nm; this treats Brownian coagulation, dry and wet depositions, in – cloud processing, condensation, evaporation, primary particle emissions and homogeneous nucleation. 	(Roldin et al., 2010a; Roldin et al., 2010b; Wang et al., 2010b)
CFD based models (e.g. StarCD, MISKAM and FLUENT codes) using RANS or LES techniques	<ul style="list-style-type: none"> • Either simulates the number and size distributions separately or the codes for simulation of particle dynamics are coupled with the CFD models. 	(Carpentieri et al., 2010; Chan et al., 2010; Gidhagen et al., 2004a; Gidhagen et al., 2003; Kumar et al., 2009b)

1523

1524 Table 3. Summary of the importance of various transformation processes at various
 1525 urban scales for consideration in dispersion models (Ketzler and Berkowicz, 2004;
 1526 Kumar et al., 2010c). Symbols +, – and 0 denotes gain, loss and no effect of the
 1527 transformation processes on ToN concentrations, respectively. Acronyms I, V and n
 1528 stand for important, very important and not important (can be ignored), respectively.

Transformation processes	Effects on concentrations		Vehicle wake		Street canyons	Neighbourhood	City	Tunnel
	number	volume	near	far				
Emissions	+	+	V	V	V	V	V	V
Nucleation	+	+	V	I	I*	I*	I	I
Dilution	+/-	+/-	V	V	V	V	V	V
Coagulation	-	0	n***	n***	n**	n**	I	V
Condensation	0	+	V	I	n**	n**	I	I
Evaporation	0/-	-	I	V	I	I	n	I
Dry deposition	-	-	V	V	I	I	I	V
Wet deposition	-	-	n	n	n	n	I	n

1529 *Important near the source (i.e. vehicle tail pipe); probably not important later though will depend
 1530 on the background concentrations, dilution and other meteorological parameters (i.e. wind speed,
 1531 direction, temperature, solar radiation).

1532 ** Depending on the background concentrations, fresh emissions and meteorological parameters;
 1533 relevant especially for sub-10 nm particles.

1534 *** Important when very small particles <10 nm are considered.

1535

1536 Table 4. Summary of PNEFs for various types of road vehicles at different speeds.

PNEF (average \pm standard deviation $\times 10^{14}$ # veh ⁻¹ km ⁻¹)	Size range covered (nm)	Average vehicle speed (km h ⁻¹)	Instruments used	Location	Author (year)
Mixed vehicle fleet (range $\sim 10^{14}$)					
2.15 \pm 0.05	10–700	90–110	DMPS	Highway, Copenhagen, Denmark	Wang et al. (2010a)
1.87 \pm 0.03	10–700	40–50	DMPS	Urban street, Copenhagen, Denmark	Wang et al. (2010a)
1.33 \pm 0.5	10–300	20–30	DMS500	Cambridge street, UK	Kumar et al. (2009b)
1.57 \pm 0.76	5–1000	\sim 30	DMS500	Cambridge street, UK	Kumar et al. (2008b)
7.9	7–3000	86 (HDVs), 116 (cars)	CPC	Haerkingen, Switzerland	Hueglin et al. (2006)
1.8 4.7	30–10000 10–400	112 (HDVs), 86 (LDVs)	SMPS–OPC SMPS	Bundesautobahn motorway, Germany	Corsmeier et al. (2005)
1.11 \pm 0.90 0.57 \pm 0.28	15–700 15–700	100 <60 (stop–start)	SMPS SMPS	Brisbane roads, Australia	Morawska et al. (2005)
3.9 11.7 13.5	>7 >7 >7	50 100 120	CPC, SMPS CPC, SMPS CPC, SMPS	Zurich roads, Switzerland	Imhof et al. (2005a)
0.96–4.7	6–220	85	-	Los Angeles motorway, USA	Zhang et al. (2005)
5.2	>6	96.6	CPC	Freeway Los Angeles, USA	Zhu and Hinds (2005)
2.8 (\pm 23%) HDVs (18.1%) 0.23 (\pm 24%) HDVs (2.7%)	15–700 15–700	100 100	SMPS–CPC	Motorway, Brisbane Australia	Gramotnev et al. (2004)
1.5 \pm 0.08	18–700	80	SMPS	Plabutsch tunnel, Austria	Imhof et al. (2005b)
1.26 \pm 0.10	18–700	64	SMPS	Kingsway tunnel, UK	
1.8 \pm 0.42	30–10000	120	ELPI	Bundesautobahn motorway, Germany	Imhof et al. (2005c)
2.7 \pm 1.1 3.3 \pm 1.4 5.4 \pm 3.4 11 \pm 5.7 4.6 \pm 1.9	30–900 30–900 30–900 30–900 30–900	70 75 80 85 70–90	DMPS DMPS DMPS DMPS DMPS	Stockholm Tunnel, Sweden	Kristensson et al. (2004)
0.87–2.73 1.93–9.94	8–300 3–1000	8–80 8–80	SMPS CPC	Minnesota roadway, USA	Kittelson et al. (2004)
2.8 \pm 0.5	10–700	40–50	CPC, DMPS	Copenhagen roads, Denmark	Ketzel et al. (2003)

	10–500		SMPS	Tuscarora Mountain Tunnel, Pennsylvania, USA	Gertler et al. (2002)
1.75 (Standard error 67.6%)	17–890	100	SMPS	On-road model estimation, Queensland Australia	Jamriska and Morawska (2001)
Heavy duty vehicles, HDVs (range ~10¹⁴–10¹⁵)					
17.5 ± 0.68	10–700	90–110	DMPS	Highway, Copenhagen, Denmark	Wang et al. (2010a)
22.06 ± 1.28	10–700	40–50	DMPS	Urban street, Copenhagen, Denmark	Wang et al. (2010a)
7.06 ± 1.81	>7	39.5	CPC	Marylebone road, London, UK	Beddows and Harrison (2008)
6.67 ± 0.91	11–437	<50	SMPS	London roads, UK	Jones and Harrison (2006)
7.8	30–10000	85.8 ± 7.5	SMPS–OPC	Motorway, Germany	Corsmeier et al. (2005)
55	>7	50	SMPS–CPC	Zurich roads, Switzerland	Imhof et al. (2005a)
69	>7	100	SMPS–CPC		
73	>7	120	SMPS–CPC		
7.79 ± 6.32	30–10000	86	ELPI	Bundesautobahn motorway, Germany	Imhof et al. (2005c)
3.23 ± 9.9	7–270	-	SMPS–CPC	Caldecott Tunnel Berkeley, USA	Geller et al. (2005)
3.9	7–450	40	DMPS–CPC	Roadside Stockholm, Sweden	Gidhagen et al. (2004a)
52	3–450	100–120	DMPS–CPC	Highway, Stockholm, Sweden	Gidhagen et al. (2004b)
73.3	3–900	48–85	DMPS	Road tunnel, Stockholm, Sweden	Gidhagen et al. (2003)
2.8 (standard deviation 10–15%)	15–700	–	SMPS	Motorway, Brisbane Australia	Gramotnev et al. (2003b)
2.1–3.1 (HDV>64%)	10–400	<90	SMPS	Tuscarora mountain tunnel, Pennsylvania, USA	Abu-Allaban et al. (2002)
0.51–0.54 (HDV 13–15%)	10–400	<90	SMPS		
Light duty vehicles, LDVs (range ~10¹³–10¹⁴)					
0.81 ± 0.07	10–700	90–110	DMPS	Highway, Copenhagen, Denmark	Wang et al. (2010a)

1.01 ± 0.06	10–700	40–50	DMPS	Urban street, Copenhagen, Denmark	Wang et al. (2010a)
0.63 ± 0.16	>7	39.5	CPC	Marylebone road, London, UK	Beddows and Harrison (2008)
0.60 ± 0.16	11–437	<50	SMPS	London roadside, UK	Jones and Harrison (2006)
0.0018 (Euro–4 with DPF)	7–10,000	50–120	ELPI	Dynamometer, Napoli, Italy	Prati and Costagliola (2008)
1.2	30–10000	111.5 ± 16	SMPS–OPC	Motorway, Germany	Corsmeier et al. (2005)
0.8	>7	50	SMPS–CPC	Zurich roads, Switzerland	Imhof et al. (2005a)
3.2	>7	100	SMPS–CPC		
6.9	>7	120	SMPS–CPC		
1.22 ± 0.49	30–10000	113	ELPI	Bundesautobahn motorway, Germany	Imhof et al. (2005c)
2.2 ± 1.24	7–270	-		Caldecott Tunnel Berkeley, USA	Geller et al. (2005)
1.4	3–450	100–120	DMPS–CPC	Highway, Stockholm, Sweden	Gidhagen et al. (2004b)
1.74	3–900	48	DMPS	Road tunnel, Stockholm, Sweden	Gidhagen et al. (2003)
10.1	3–900	85			
Cars (petrol–fuelled) (range ~10¹²–10¹⁴)					
0.03–1.3	>10	50, 70	CPC	Gothenberg road, Sweden	Hak et al. (2009)
~0.017	7–400	30	SMPS	Leipzig road, Germany	Wehner et al. (2009)
~0.018	7–400	95	SMPS		
~0.074	7–400	150	SMPS		
0.0234 (Euro–2 and Euro–3)	7–10,000	50–120	ELPI	Dynamometer, Napoli, Italy	Prati and Costagliola (2008)
0.17–0.45	11–450	<50	SMPS	London, UK	Jones and Harrison (2006)
0.189 ± 0.34	15–700	100	SMPS	Brisbane, Australia	Morawska et al. (2005)
0.218 ± 0.06	15–700	<60 (stop–start)	SMPS		
Cars (diesel–fuelled) (range ~10¹⁴)					
1.4–1.8	>10	50, 70	CPC	Gothenberg roads, Sweden	Hak et al. (2009)
~1.6 (Urban roads)	7–400	30	SMPS	Leipzig urban roads and freeways, Germany	Wehner et al. (2009)
~0.6 (low engine load)	7–400	105	SMPS		
~4.2 (high engine load)	7–400	105	SMPS		
~1.1 (low engine load)	7–400	120	SMPS		
~1.3 (medium engine load)	7–400	149	SMPS		

~4.4 (high engine load)	7–400	149	SMPS		
1.32 (Euro-3; without DPF)	7–10,000	50–120	ELPI	Dynamometer, Napoli, Italy	Prati and Costagliola (2008)
0.44	8–400	50	SMPS	Delft, Netherlands	Rijkeboer et al. (2005)
0.57	8–400	70	SMPS		
1 (all results for steady state conditions)	8–400	100	SMPS		
7.17 ± 2.80	15–700	100	SMPS	Brisbane roads, Australia	Morawska et al. (2005)
2.04 ± 0.24	15–700	<60 (stop–start)	SMPS		
Buses (diesel-fuelled) (range ~10¹⁴)					
1.2 (25% engine power)	5–4000	60	SMPS–CPC	Dynamometer, Brisbane Australia	Jayaratne et al. (2009)
1.5 (50% engine power)	5–4000	60	SMPS–CPC		
18 (100% engine power)	5–4000	60	SMPS–CPC		
3.11 ± 2.41	17–700	60	SMPS	Woolloongabba Tunnel, Brisbane Australia	Jamriska et al. (2004)
3.87 ± 2.49	8–400	40–80	SMPS	Dynamometer, Brisbane Australia	Ristovski et al. (2002)
1.57	8–304	80	SMPS	Dynamometer, Brisbane Australia	Morawska et al. (1998)
Buses (compressed natural gas; CNG) (range ~10⁰⁸– 10¹⁵)					
0.10 (25% engine power)	5–4000	60	SMPS–CPC	Dynamometer, Brisbane Australia	Jayaratne et al. (2009)
0.25 (50% engine power)	5–4000	60	SMPS–CPC		
14 (100% engine power)	5–4000	60	SMPS–CPC		
~0.00015–0.0003 (load 6.5 kW)	5–400	40	SMPS	Dynamometer, Brisbane Australia	Ristovski et al. (2004)
~0.00006–0.0003 (load 9.5 kW)	5–400	60	SMPS		
~0.000007–0.15 (load 12.5 kW)	5–400	80	SMPS		
~0.05–0.16 (load 18.8 kW) (all results for 6 cylinder SI engine)	5–400	100	SMPS		
Petrol-fuelled spark ignited vehicles (range ~10⁹– 10¹³)					
~0.000076–0.15 (load 6.5 kW)	5–400	40	SMPS	Dynamometer, Brisbane Australia	Ristovski et al. (2004)
~0.00008–0.15 (load 9.5 kW)	5–400	60	SMPS		
~0.0003–0.1 (load 12.5 kW)	5–400	80	SMPS		
~0.2–0.21 (load 18.8 kW)	5–400	100	SMPS		

kW)					
(all results for 6 cylinder SI engine)					
~0.08	8–400	40	SMPS	Dynamometer,	Ristovski et al.
~0.02	8–400	60	SMPS	Brisbane	(2005)
~0.20	8–400	80	SMPS	Australia	
~0.50	8–400	100	SMPS		
(all results for LPG 4 1, 6 cylinder SI engine fuelled by unleaded petrol)					
Light petroleum gas, LPG-fuelled spark ignited vehicles (range $\sim 10^{10}$–10^{12})					
~0.0009	8–400	40	SMPS	Dynamometer,	Ristovski et al.
~0.008	8–400	60	SMPS	Brisbane	(2005)
~0.05	8–400	80	SMPS	Australia	
~0.08	8–400	100	SMPS		
(all results for LPG 4 1, 6 cylinder SI engine)					
Vehicles generated through road–tyre interface (range $\sim 10^{11}$–10^{12})					
0.0037	15–700	50	SMPS–DMA	Road simulator,	Dahl et al.
0.032	15–700	70	SMPS–DMA	Transport	(2006)
(most particles in 15–50 nm size range)				Research	
				Institute,	
				Sweden	
Two-wheelers (range $\sim 10^{14}$–10^{15})					
0.31 (2–stroke; Euro–1 and Euro–2)	7–10,000	20–45	ELPI	Dynamometer,	Prati and
0.10 (4–stroke; Euro–1 and Euro–2)	7–10,000	20–45	ELPI	Napoli, Italy	Costagliola
1.9–4	8–400	30	SMPS	Delft,	Rijkeboer et al.
21	8–400	50	SMPS	Netherlands	(2005)
11	8–400	70	SMPS		
7.5	8–400	90	SMPS		
(2–stroke motorcycles; values are in # km ⁻¹ at peaks $dN(d\log D_p)^{-1}$)					

- 1537 DMS = differential mobility spectrometer, SMPS = scanning mobility particle sizer,
1538 CPC = condensation particle counter, DMPS = differential mobility particle sizer,
1539 EAA = electrical aerosol sizer, UCPC = ultrafine condensation particle counter, ELPI
1540 = electrical low pressure impactor

Fig.1.ppt_ABL

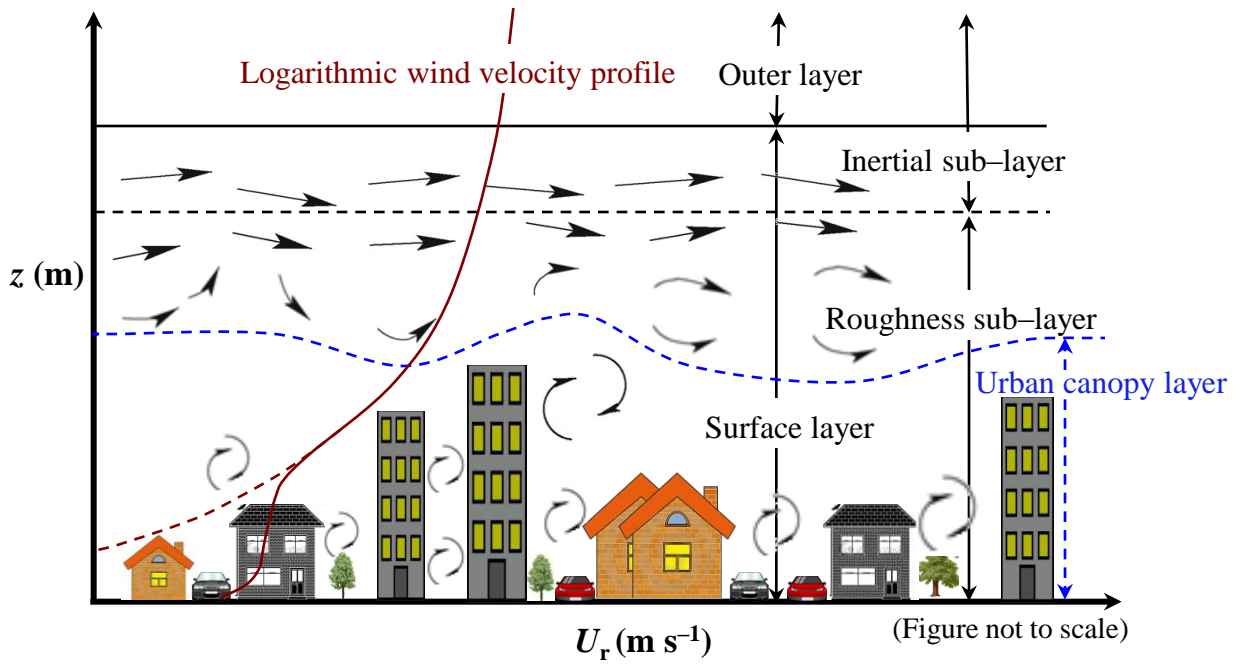


Fig. 2.ppt_Dry Deposition

- ◇ $u^* = 133 \text{ cm/s}$; $1/ra = 3 \text{ cm/s}$ (Seinfeld and Pandis, 2006)
- ◆ $u^* = 50 \text{ cm/s}$; $1/ra = 3 \text{ cm/s}$ (Seinfeld and Pandis, 2006)
- $u^* = 133 \text{ cm/s}$; $z_0 = 0.13 \text{ cm}$ (Schack et al., 1985)
- $u^* = 133 \text{ cm/s}$; $z_0 = 1 \text{ cm}$ (Schack et al., 1985)
- $u^* = 27 \text{ cm/s}$; $z_0 = 0.13 \text{ cm}$ (Schack et al., 1985)
- ▲ vs (Seinfeld and Pandis, 2006)

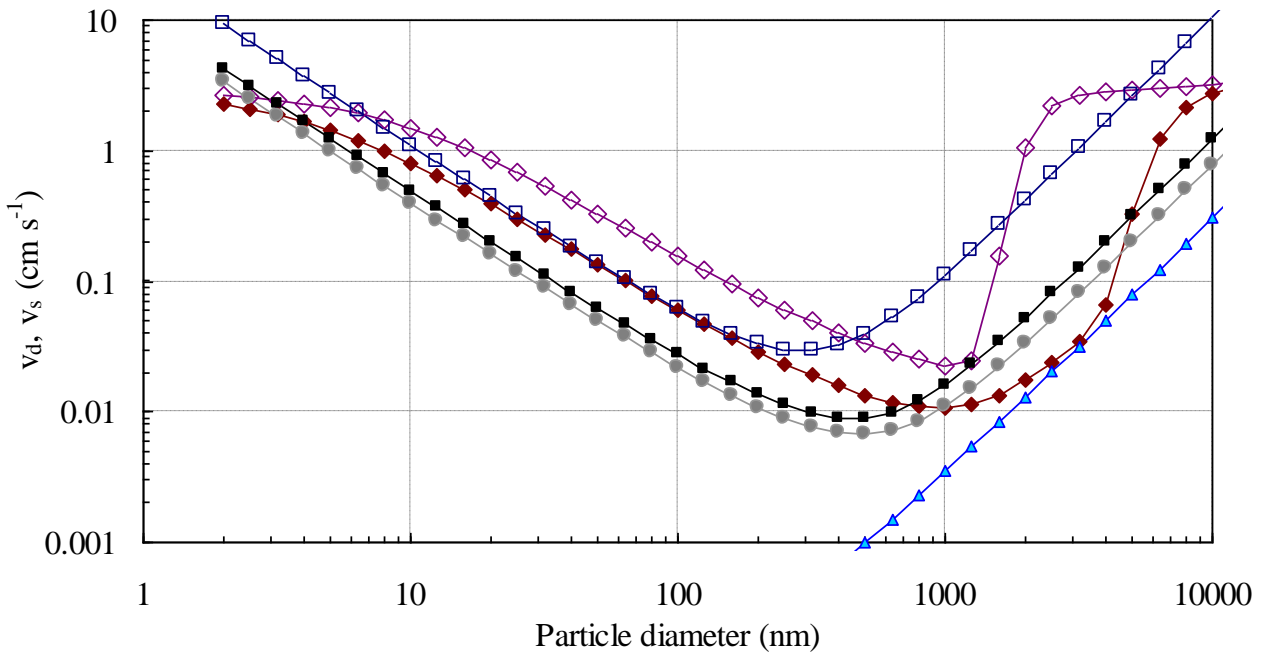


Fig. 3.ppt_Time Scales

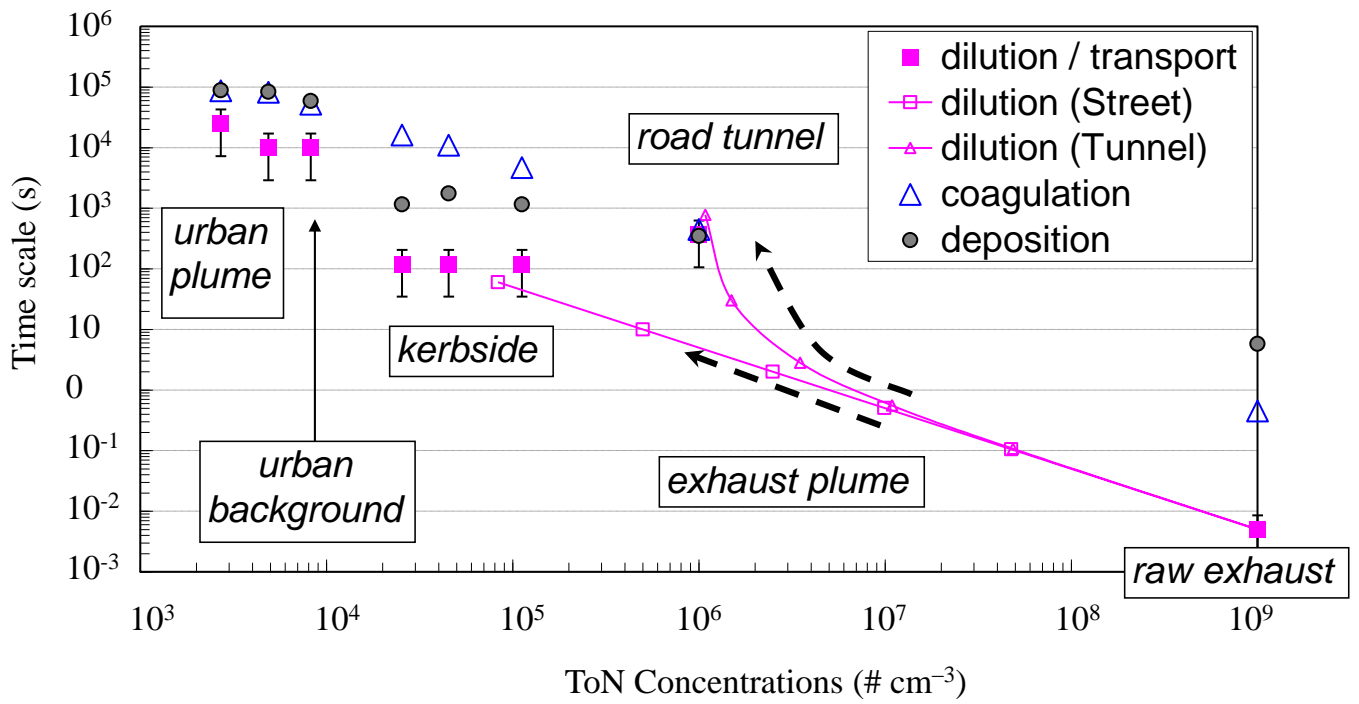


Fig. 4.ppt_PNDs at Different heights

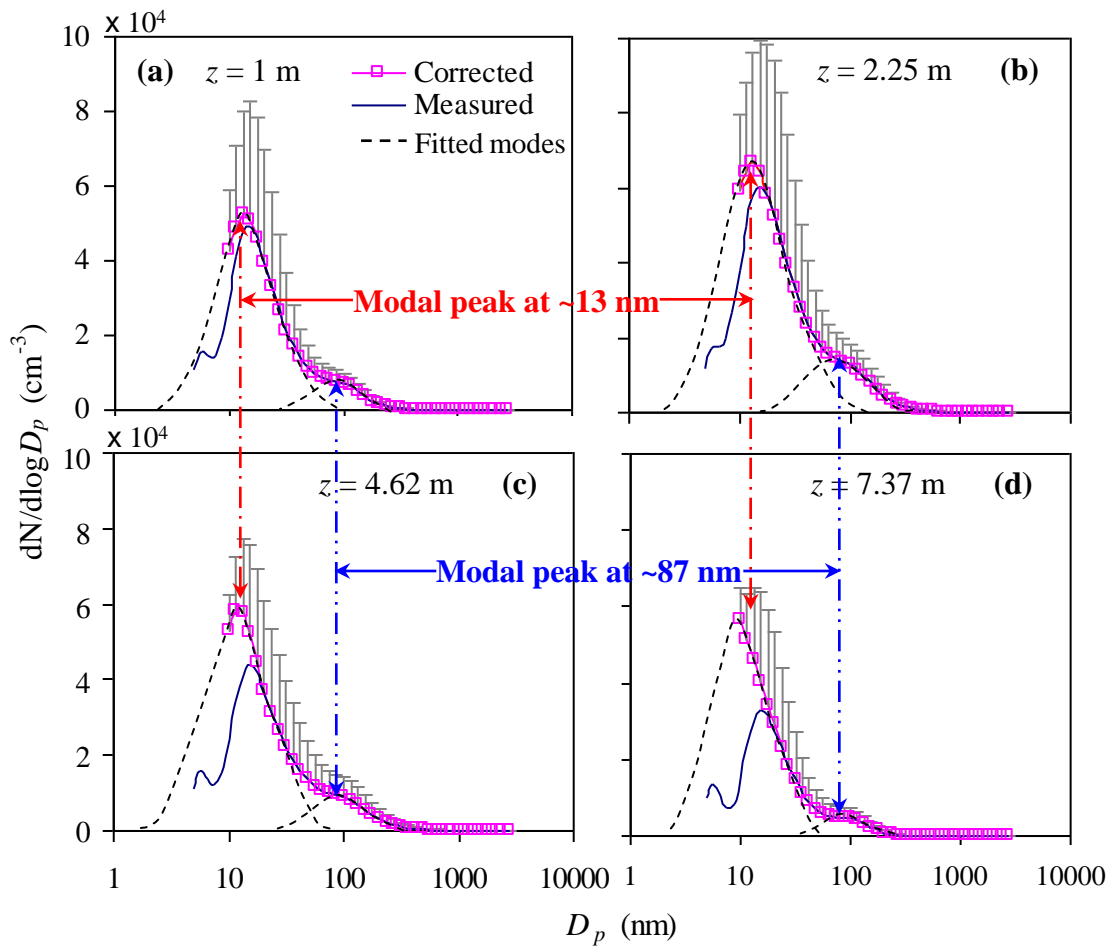
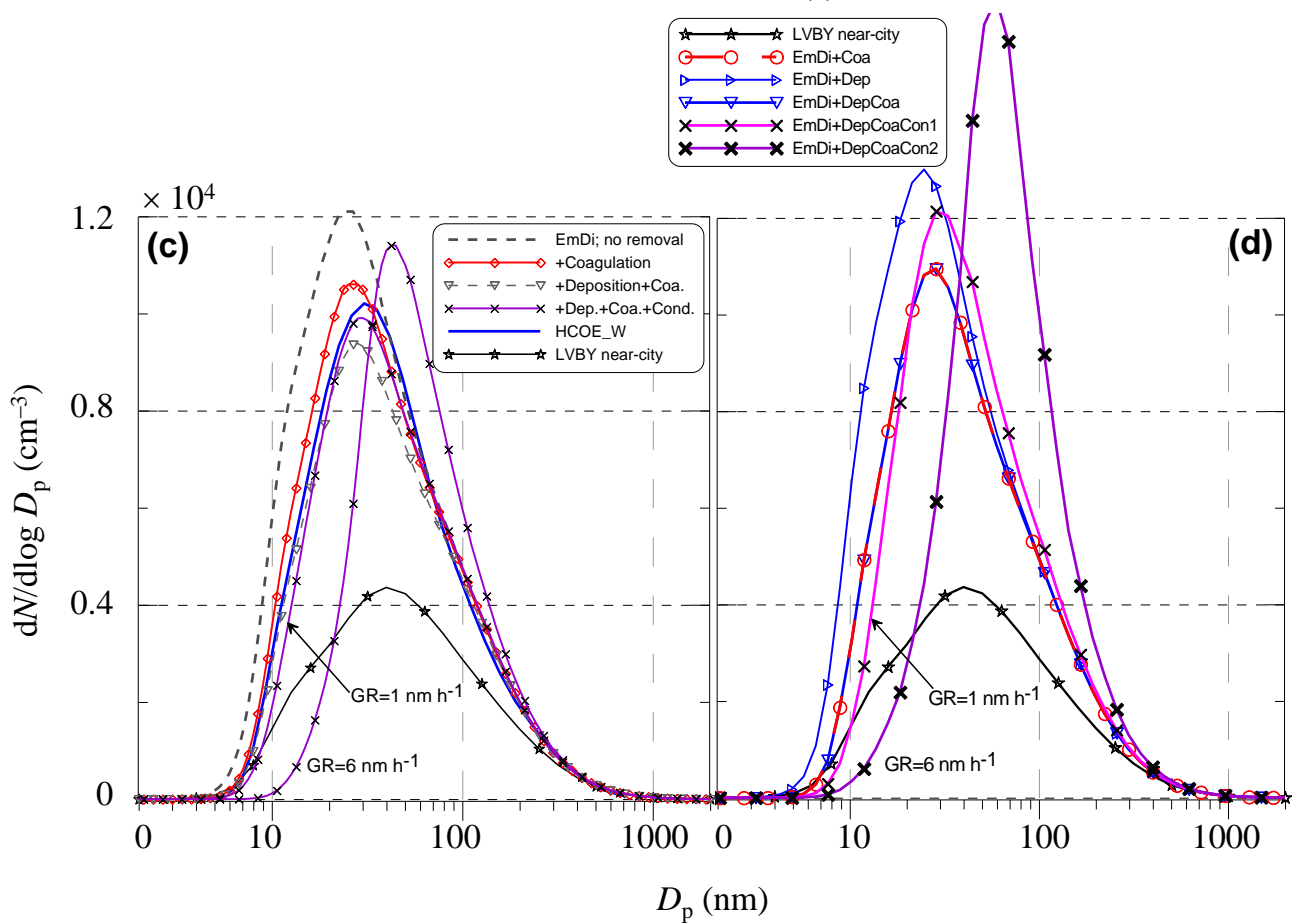
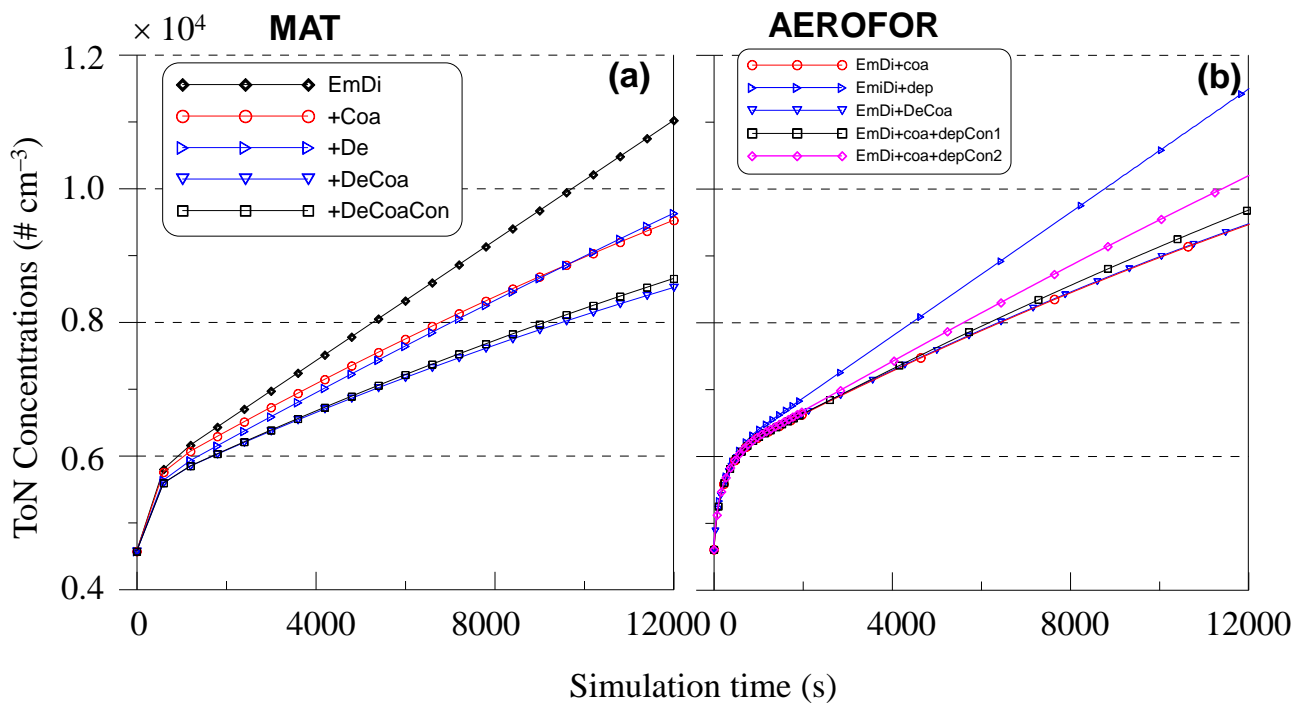


Fig. 5.ppt_Modelling Results



Please cite this article as:

Kumar, P., Ketzler, M., Vardoulakis, S., Pirjola, L., Britter, R., 2011. Dynamics and dispersion modelling of nanoparticles from road traffic in the urban atmospheric environment - a review. *Journal of Aerosol Science* 42, 580-603.